Proposal: MAKAH-GWU-0812
Period of Award: 8/1/12 – 12/31/12

The purpose of this proposed statement of work (SOW) is to develop a geographic profile for oil spill risk using the MTS risk simulation methodology described in Appendix A for the year 2010. Appendix A describes the methodology for such an analysis for the year 2005 (specifically for the period from 03/01/05 to 02/28/06). Figure 1 (included in Appendix A) is such a geographic oil spill risk profile for the year 2005.

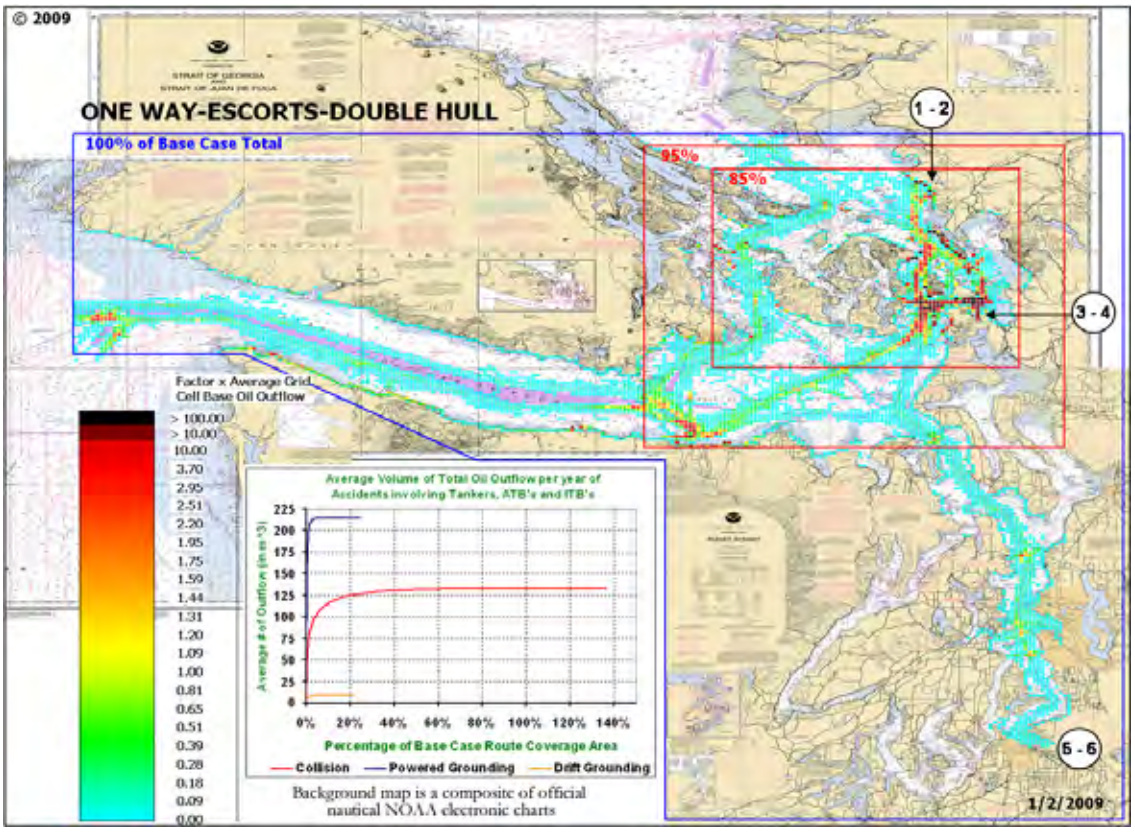

Figure 1. Geographic oil outflow profile explaining MTS oil spill system risk developed using 2005 Vessel Traffic Operational Support System (VTOSS) data.

The proposed analysis will modify/update the MTS risk simulation presented in Appendix A using 2010 VTOSS data only. All other aspects in this MTS risk simulation will remain the same for the purpose of this analysis. See Figure 2 for the geographic coverage area of VTOSS data.

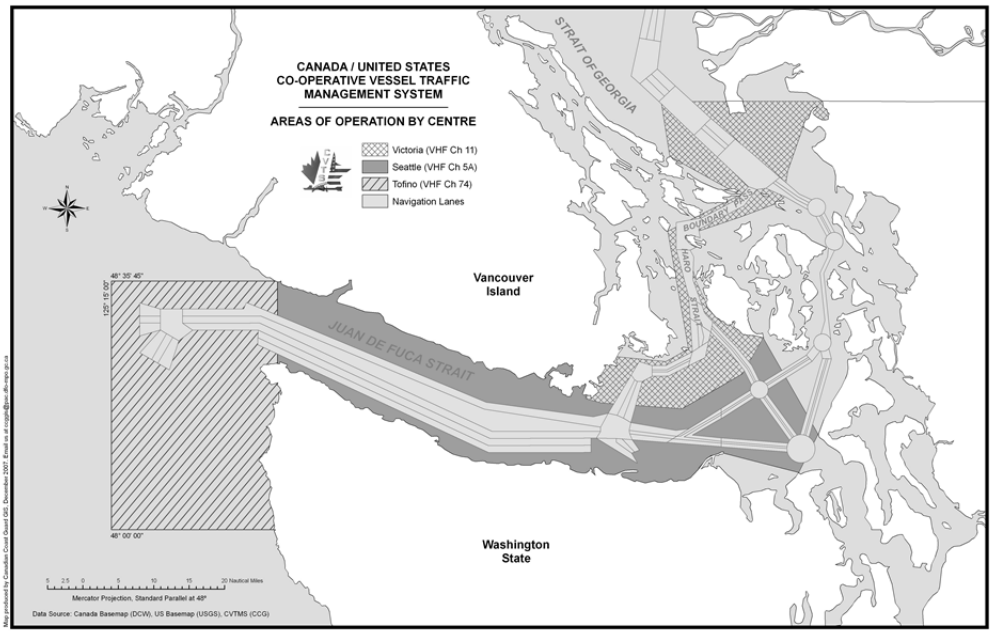

Figure 2. Geographic Coverage of (VTOSS) data.

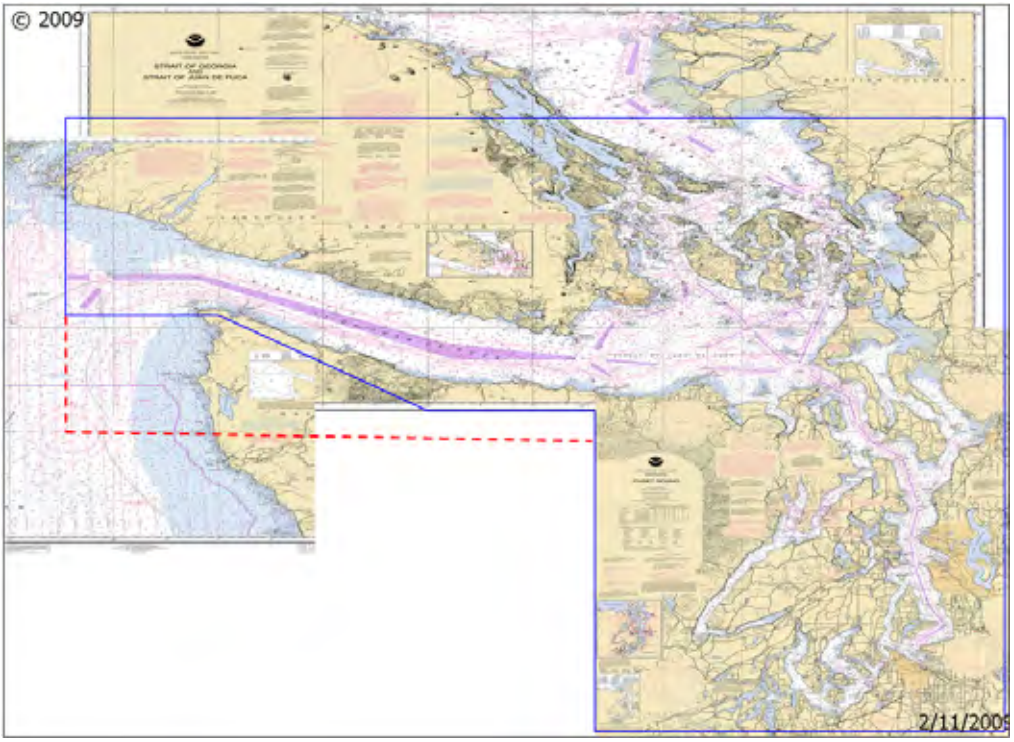

Figure 3. Geographic Coverage of (VTOSS) data.

The geographic area for the 2010 analysis will be expanded as compared to Figure 1 as indicated in Figure 3. This effectively means that the 2010 analysis will cover the complete VTOSS geographic coverage area. Retaining "blue corner points" will allow for a comparison of 2010 analysis to the 2005 analysis in Figure 1 by location. Location definition for the 2010 analysis is provided in Figure 4. The blue "West Strait of Juan de Fuca Area" will be expanded up to the dotted red line in Figure 3.

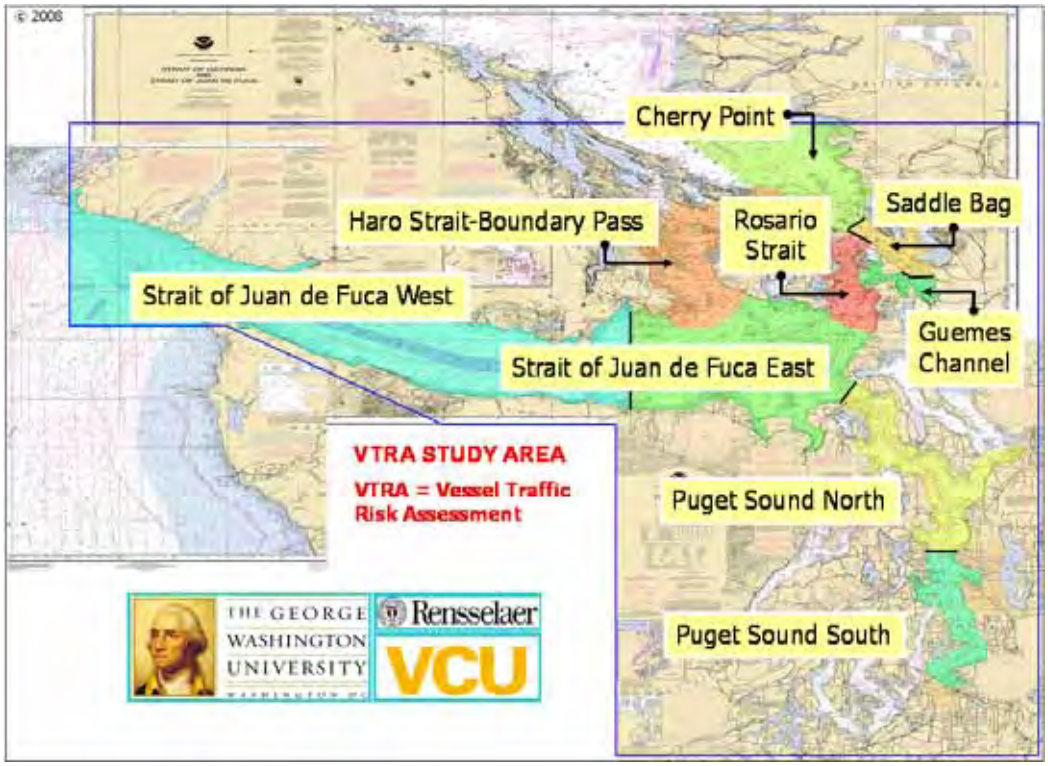

Figure 4. Location Definition in VTRA Study.

The 2010 geographic profile oil spill risk to be developed will use the analysis in Figure 1 as its base case for comparison purposes. A visual comparison of both profiles will indicate geographic changes in oil spill risk by location from the 2005 analysis to the 2010 analysis. In addition, analysis results will be presented in the format of Table 1 (also included in Appendix A). The acronym VOI in Table 1 stands for vessel of interest and the acronym interacting vessel stand for interacting vessel. As in Appendix A VOI's shall be tankers, articulated tug barges, and integrated tug barges which transport both crude oil and refined products in the study area reflected in Figure 1. It shall be assumed for the 2010 analysis all VOI's have double hulls (at the time of the study some of them were still phased in). The northerly route (through Rosario Strait) towards Refineries 1 and 2 is classified as a one way zone for certain larger vessels. An escorting regime for escorting laden tank vessels was implemented in the MTS simulation that mimics the current escorting operations within that study area. The crude cargo and bunker fuel are called persistent oil (PO) since they are "heavier" and less volatile than refined products and diesel fuel. Refined products and diesel fuel shall be referred to as non-persistent oil (NPO). Considering further the VOI or IV origin of the potential oil losses the following four categories are listed in Table 1: VOI PO, VOI NPO, IV PO and IV NPO.

Table 1. Total overage annual oil outflow (in separated by persistent oil (PO) and non-persistent oil (NPO) by VOI's, IV's and accident type.

in m^3	VOI PO	VOI NPO	IV PO	IV NPO	Total Outflow
Collisions	109.82	12.35	2.06	9.47	133.71
Powered Groundings	208.62	9.73	N/A	N/A	218.35
Drift Groundings	8.39	0.52	N/A	N/A	8.91
Total Outflow	326.82	22.61	2.06	9.47	360.96

in % of Total Outflow	VOI PO	VOI NPO	IV PO	IV NPO	Total Outflow
Collisions	30.42%	3.42%	0.57%	2.62%	37.04%
Powered Groundings	57.79%	2.70%	N/A	N/A	60.49%
Drift Groundings	2.32%	0.14%	N/A	N/A	2.47%
Total Outflow	90.54%	6.26%	0.57%	2.62%	100.00%

Table 2. Vessel Type and Location Classification for 2010 Tabular Analysis.

LOCATION
Cherry Point Area
Puget Sound South
Strait of Juan de Fuca East
Strait of Juan de Fuca West
Puget Sound North
Saddle Bag Area
Rosario Strait
Haro Strait\Boundary Pass
Guemes Channel

VESSEL TYPE
Tug without Barge
Tug ATB's or ITB's
Tug Pushing Ahead
Container
Tanker
Bulk carrier
Freighter
Passenger vessel
Service vessel
Public vessel
Fishing Vessel
Tug Towing Astern
Recreational Vessel

A tabular exposure comparison will be provided between 2005 and 2010 in terms of the location and vessel type classification provided in Table 2. This comparison will be provided for the "enlarged" West-Strait of Juan de Fuca area as explained above. With respect to the Tug category further refinement in terms of type of cargo will be provided to the extend the 2010 VTOSS data provides that information.

In addition, a separate geographic exposure/traffic density profiles analysis shall be developed for an agreed upon taxonomy of the vessel classes modeled in the maritime simulation. This analysis will further identify/highlight changes in vessel traffic from 2005 to 2010. Such an analysis is informative for the development of potential risk mitigation strategies targeting changes in traffic

that have occurred or may occur in the future. The 26 different vessel types modeled in the MTS simulation are listed in Table 3. A separate power point presentation shall be developed comparing 2005 geographic traffic density profiles to those of 2010.

Table 3. Vessel Types for geographic profile/traffic density analysis of 2010 traffic.

	Vessel Type		Vessel Type		Vessel Type
1	BULKCARRIER	11	OILTANKER	21	USCOASTGUARD
2	CHEMICALCARRIER	12	OTHERSPECIALCARGO	22	VEHICLECARRIER
3	CONTAINERSHIP	13	OTHERSPECIFICSERV	23	YACHT
4	DECKSHIPCARGO,	14	PASSENGERSHIP	24	ATB
5	FERRY	15	REFRIGERATEDCARGO	25	ITB
6	FERRYNONLOCAL	16	RESEARCHSHIP	26	OILBARGE
7	FISHINGFACTORY	17	ROROCARGOSHIP		
8	FISHINGVESSEL	18	ROROCARGOCONTSHIP		
9	LIQGASCARRIER	19	SUPPLYOFFSHORE		
10	NAVYVESSEL	20	TUGTOWBARGE		

A final report describing the analysis results shall be produced as part of this statement of work providing a detailed analysis of the geographic profiles of 2005 and 2010 oil spill system risk and tabular exposure analysis by vessel type and location for the classes described in Table 2. The graphic traffic density presentation shall serve as an appendix of the final report.

Principal Investigator for this statement of work shall be Johan Rene van Dorp. The traffic update modeling for the MTS simulation will be performed by Jason Merrick (VCU) under a subcontract from GWU to VCU. The level of effort for GWU for this SOW is estimated at 93.5% month and level of effort for Jason Merrick is at the equivalent of one and a half course buyout at VCU for the Fall 2012 semester. A budget is attached totaling $74,873 for this effort.

Attachments: MAKAH-GWU-0812

Appendix A:

Van Dorp, J.R. and Merrick, J.R.W. (2011). On a risk management analysis of oil spill risk using maritime transportation system simulation, *Annals of Operations Research* (2011) 187:249–277

Appendix B:

The George Washington University Administrative Data Sheet

Appendix C:

A copy of a Facilities and Administrative Rate Agreement

Appendix D: Subcontract VCU to GWU:

Vessel Traffic Risk Assessment Simulation Data Update to 2010 – A proposal from VCU submitted to GWU

Appendix A:

Van Dorp, J.R. and Merrick, J.R.W. (2011). On a risk management analysis of oil spill risk using maritime transportation system simulation, Annals of Operations Research (2011) 187:249–277

Ann Oper Res (2011) 187:249–277
DOI 10.1007/s10479-009-0678-1

On a risk management analysis of oil spill risk using maritime transportation system simulation

J. René van Dorp · Jason R.W. Merrick

Published online: 12 December 2009

Abstract Is it safer for New Orleans river gambling boats to be underway than to be dockside? Is oil transportation risk reduced by lowering wind restrictions from 45 to 35 knots at Hinchinbrook Entrance for laden oil tankers departing Valdez, Alaska? Should the International Safety Management (ISM) code be implemented fleet-wide for the Washington State Ferries in Seattle, or does it make more sense to invest in additional life craft? Can ferry service in San Francisco Bay be expanded in a safe manner to relieve high way congestion? These risk management questions were raised in a series of projects spanning a time frame of more than 10 years. They were addressed using a risk management analysis methodology developed over these years by a consortium of universities. In this paper we shall briefly review this methodology which integrates simulation of Maritime Transportation Systems (MTS) with incident/accident data collection, expert judgment elicitation and a consequence model. We shall describe recent advances with respect to this methodology in more detail. These improvements were made in the context of a two-year oil transportation risk study conducted from 2006–2008 in the Puget Sound and surrounding waters. An application of this methodology shall be presented comparing the risk reduction effectiveness analysis of a one-way zone, an escorting and a double hull requirement in the same context.

Keywords Risk management analysis · Maritime transportation system · Simulation · Expert judgment elicitation · Oil outflow analysis

1 Introduction

The National Research Council (1986, 1991, 1994, 2000, 2001) has repeatedly identified the assessment and management of risk in maritime transportation as an important prob-

J.R. van Dorp (✉)
Department of Engineering Management and Systems Engineering, The George Washington University, Washington, USA
e-mail: dorpjr@gwu.edu

J.R.W. Merrick
Department of Statistical Sciences & Operations Research, Virginia Commonwealth University, Richmond, USA

lem domain. In earlier work, researchers concentrated on assessing the safety of individual vessels or marine structures, such as nuclear powered vessels (Pravda and Lightner 1966), vessels transporting liquefied natural gas (Stiehl 1977), and offshore oil and gas platforms (Paté-Cornell 1990). The United Stated Coast Guard (USCG) has used a classical statistical analysis of nationwide accident data to prioritize federal spending in order to improve port infrastructures (USCG 1973 and Maio et al. 1991).

More recently, researchers have used probabilistic risk assessment (PRA) (Bedford and Cooke 2001) in the maritime domain by examining risk in the context of maritime transportation systems (Hara and Nakamura 1995; Roeleven et al. 1995; Kite-Powell et al. 1996; Slob 1998; Fowler and Sorgard 2000; Trbojevic and Carr 2000; Wang 2000; GuedesSoares and Teixeira 2001). In a maritime transportation system (MTS), (NRC 2000) traffic patterns change over time in a complex manner. Researchers have used system simulation as a modeling tool to assess MTS service levels (Andrews et al. 1996), to perform logistical analysis (Golkar et al. 1998), and to facilitate the design of ports (Ryan 1998). The dynamic nature of traffic patterns in a port and of other situational variables, such as wind, visibility, current, and ice, implies that risk is a dynamic quantity that changes over time. Implementing new traffic rules in an MTS alter traffic patterns, and thus also its risk behavior. Such a change in risk behavior within an MTS can be assessed ahead of time through the use of simulation models. In fact, the questions in the abstract have all been addressed using the same risk management analysis methodology involving a dynamic risk simulation of MTS's. This methodology has been developed and continuously improved over a span of more than 10 years by primarily three U.S. universities: The George Washington University, Virginia Common Wealth University, Rensselear Polytechnic Institute, and most recently also involved the Delft University of Technology, The Netherlands. A separate team of researchers from Rutgers University and Bogacizi University, Turkey, adopted a version of this methodology to assess vessel traffic risk in the Strait of Istanbul (Ulusçu et al. 2009).

In Sect. 2 we shall present an overview of the risk management analysis methodology described in more detail in Merrick et al. (2000, 2001, 2002, 2003) and van Dorp et al. (2001). This methodology centers around a causal chain analysis (depicted in Fig. 1) that integrates maritime transportation simulation with an accident probability model and a consequence model. Expert judgment elicitation and historical incident/accident data serve as the information sources to estimate accident probability model parameters. The final analysis layer is a consequence model that may draw from naval architect type arguments. The consequence metric of interest depends on the context of a particular study. Herein, the consequence analysis is measured in terms of volume of oil spilled from tank vessels. We shall use this paper to highlight some recent advances of the above three aspects of this dynamic risk management analysis methodology, but also use it to present an improved graphical format to represent maritime transportation risk in a geographic manner. These enhancements were made during a vessel oil transportation risk assessment study from 2006–2008 in the Puget Sound and surrounding waters. The oil transportation routes in question traverse the San Juan Islands and the Straits of Juan de Fuca. The San Juan Islands area is considered an environmentally pristine area and serves as a habitat for an orca whales family. Moreover, the San Juan Islands and the Strait of Juan de Fuca are fishing grounds for both commercial and tribal salmon, crab, and shrimp fisheries.

Section 3 details improvements with respect to constructing a more representative and detailed maritime simulation. In Sect. 4, we report on an enhanced grounding accident frequency model that now includes a time-to-shore variable. Intuitively, longer times-to-shore result in reduced grounding probabilities. In Sect. 5, an augmentation of an oil outflow model is presented that builds on 80,000 physical simulation scenarios of collisions and groundings

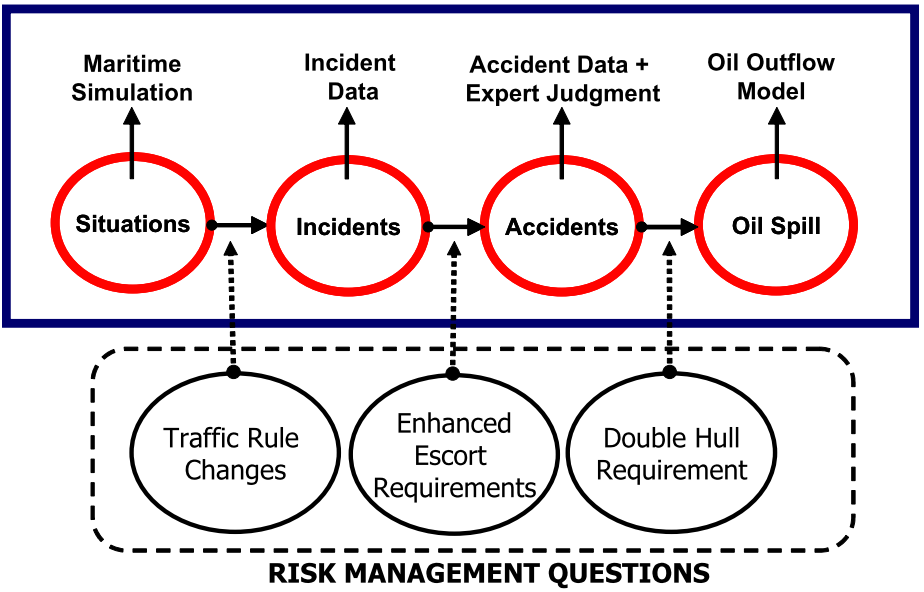

Fig. 1 Causal chain of events interconnected by causal pathways. Risk management questions attempt to block these causal pathways

conducted during a National Research Council study (NRC 2001). It (a) explicitly links a vessel's longitudinal and transversal damage extent to kinetic energy principles, (b) was constructed keeping computational efficiency in mind, and (c) accommodates the evaluation of fuel losses besides cargo losses. In Sect. 6, we shall illustrate the risk assessment procedure by evaluating an aggregate baseline level of oil spill risk and its geographic profile for the Puget Sound and surrounding waters. Finally, in Sect. 7, we shall exemplify our risk management analysis procedure by evaluating the effectiveness of the three risk interventions measures displayed in Fig. 1 in the same geographic context.

2 Maritime transportation system risk model

In his by now classical paper entitled "The Words of Risk Analysis", Kaplan (1997) provides a definition for "system risk" as the complete set of triplets

$$\{(s_i, l_i, c_i)\}_c, \quad i = 1, 2, 3, \ldots \tag{1}$$

where s_i describes the context of an accident scenario, l_i is the likelihood of an accident occurring in that scenario and c_i is a description of the consequences associated with it. To arrive at a comprehensive understanding of a baseline level of system risk, Kaplan urges that the complete set of triplets (indicated by the subscript c in (1)) ought to be pursued.

The risk management methodology presented in this paper attempts to arrive at such an understanding of baseline risk in a maritime transportation system (MTS) by using a maritime simulation to generate and count accident scenarios s_i therein. In a nutshell, the simulation moves vessels of various types along constructed vessel routes across a nautical map following applicable traffic rules. Vessels typically report to a Vessel Traffic Service

(VTS) and arrive in the MTS simulation as per electronic data obtained from such a VTS. The MTS simulation also has built in it an hourly simulation of environmental variables such as wind, visibility and, recently, currents. Merrick et al. (2000, 2003) describe in more detail the construction of such a maritime simulation which has been coded over time directly in Pascal and does not use a pre-existing simulation platform. Each generated accident scenario is recorded to a database describing its accident and consequence descriptors, accident type and incident type preceding the accident. Incident types considered are propulsion failure, steering failure, navigational aid failure, nearby vessel failure, and human error. Accident types considered are collisions and groundings. Those groundings preceded by a steering or propulsion failure may be further classified as drift groundings and those preceded by human error, navigational aid or nearby vessel failures as powered groundings.

The likelihood l_i of an accident in scenario s_i is next evaluated using a comprehensive historical incident and accident analysis supplemented with expert judgment elicitations. While depending on data availability, incident rates of mechanical failures, and human error may be established via a historical analysis of incident data, accident databases for a specified geographic study area, thankfully, contain fewer entries. As a result accident databases may not allow for a sufficient differentiation amongst the likelihoods l_i of accident scenarios s_i in (1) via a classical statistical means. Moreover, a collision accident report may, e.g., not describe if the accident in question involved a meeting, overtaking or crossing situation of vessels, whereas this certainly would be an important descriptor for the evaluation of the accident likelihood l_i. Hence, to arrive at an accident probability model with a higher level of detail, relative accident likelihoods are elicited via a paired comparison expert judgment elicitation technique. Experts in the case of a maritime risk model are pilots, captains and first mates that have extensive experience sailing the study area in question. A data analysis of the expert responses allows us to estimate an effect of the type of interaction (i.e. meeting, crossing or passing) on the accident probability, but also of other accident descriptors such as interacting vessel type, wind, visibility, etc. (See Merrick et al. 2005 and Szwed et al. 2006 for a full description of the inference procedure.)

A metric to measure consequences c_i depends on preferably a preset definition of risk suited for the problem context in question. However, its dimension may also be driven in part by data availability. For example, during the Washington State Ferry risk assessment (van Dorp et al. 2001) a lack of passenger data necessitated a surrogate measure of passenger risk that was not rooted in the number of casualties, but defined in terms of the length of time to respond to an accident. When evaluating oil transportation risk, which is the focus of this paper, consequences c_i may be described in terms of the volume of oil spilled using naval architect type arguments (NRC 2001). Oil spill analysis results may be further separated into multiple categories, such as, e.g., crude oil, refined products, bunker fuel, and diesel fuel. Crude oil and bunker fuel are less volatile and typically display a more environmentally persistent behavior than refined products and diesel fuel. Section 5 herein describes in more detail an oil outflow model to evaluate potential cargo and vessel fuel losses.

In principle, one arrives at a metric of overall baseline system risk using (1) by evaluating

$$R_0 = \sum_{\text{all } i} l_i \times c_i, \tag{2}$$

where the summation (2) is conducted over the various incident types and accident types being considered. Risk interventions may impact the level of baseline risk R_0 in a variety of ways. For example, the "traffic rule changes" measure depicted in Fig. 1 alters the set of scenarios, the "enhanced escorting requirement" alters the likelihood of an accident, and the

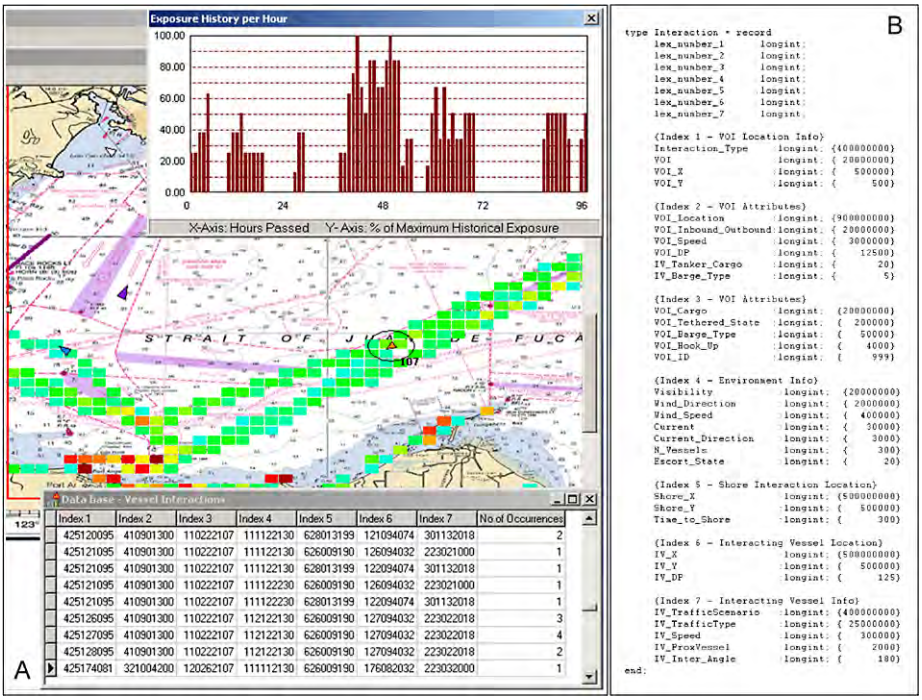

Fig. 2 (**A**) A snapshot of the scenario recording pre-processing step for a vessel of interest with id #107; (**B**) Scenario record definition

"double hull requirement" impacts the amount of oil outflow given an accident has occurred. Summarizing, going from left to right in Fig. 1, the risk intervention measures depicted impact the scenarios s_i, the likelihoods l_i and the consequences c_i in (1), respectively. Of these three measures only the "traffic rule changes" intervention measure requires a regeneration of set of scenarios s_i. The individual effect of the other two may be conducted using the same set of scenarios generated to establish baseline risk R_0 (2).

The MTS risk simulation methodology allows for the effectiveness evaluation of a simultaneous implementation of all three risk interventions measures. In general, effectiveness of a portfolio of risk interventions is unlikely to equate the sum of the individual evaluated effectiveness of members within it. Moreover, synergistic effects of a group of risk intervention measures could lead to unintended consequences. For example, the simultaneous implementation of 162 planned risk intervention measures in the PWS risk assessment analysis (Merrick et al. 2000) led to an evaluated oil transportation risk of zero, but also brought oil transportation throughput in the simulation to a grinding halt. MTS simulations are a natural platform to test for potential synergistic effects of the implementation of a set of risk interventions.

Figure 2 provides a snapshot of the MTS simulation scenario recording process. In Fig. 2A a vessel of interest (VOI) with ID #107 traverses a study area that is discretized using a $\frac{1}{2} \times \frac{1}{2}$ nautical mile grid overlain on a nautical map. VOI's in case of Fig. 1 are vessels that transport oil products on a regular basis. Specifically we consider in Sects. 6 and 7: tankers, articulated tug barges (ATB's) and integrated tug barges (ITB's). After every simulation minute, a complete snapshot is taken of the MTS and each scenario involving

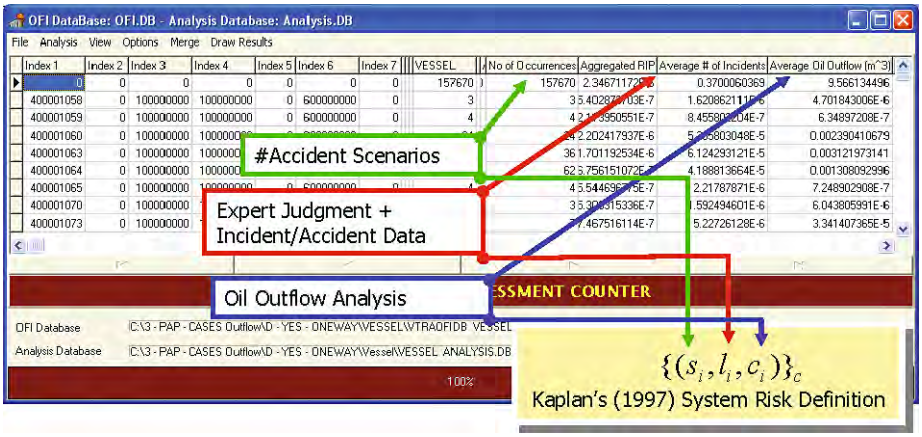

Fig. 3 A snapshot of the post-processing analysis step using a generated scenario database as input

a VOI in that snapshot is recorded. Scenario grid coordinates, accident and consequence descriptors are encoded and stored in a database using seven indices. Example accident and consequence descriptors that are recorded are: the proximity of an interacting vessel (IV), the IV type and speed, the VOI's location and speed, their interaction angle, the time to shore of the VOI, but also environmental variables, such as wind, current and visibility. Repetitions of the same scenario are counted utilizing a lexicographic ordering of these seven indices (see Fig. 2A). A VOI's id is also recorded and later used to read from file its hull configuration (single-hull or double-hull), its lightweight tonnage and full-load deadweight tonnage (DWT). Both tonnages are required to evaluate a VOI's displacement given its cargo load. A VOI's cargo load, displacement and speed, an IV's displacement and speed, and their interaction angle are needed to evaluate a VOI's damage extent, assuming it is the struck vessel. Figure 2B shows the complete record definition of the seven indices. Summarizing, the simulation of the MTS acts as a pre-processor that records and counts scenarios for (1).

A separate post-processing or querying tool depicted in Fig. 3 was developed. It uses a generated database of accident scenarios as input and overlays the incident, accident and oil outflow causal chain analysis (Fig. 1) by decoding each scenario and using its accident and consequence descriptors to evaluate its incident rate, its accident rate and oil outflow. The separation of the analysis process into a simulation pre-processor and an analysis post-processor follows as a requirement of achieving computational efficiency. To illustrate,the analysis of the baseline system risk analysis described in Sect. 6 generated 157,670 collision scenarios (see Fig. 3B) and 1,236,603 grounding accident scenarios. It took about 15 hours of runtime on a Sun Ultra work station with a 64 bit operating system to generate a database of accident scenarios to evaluate base case risk (1) for a one-year MTS simulation described in Sect. 6. A single post-processing analysis step using this database as input took about four hours of runtime. Needless to say these generation/calculation times depend not only on the geographic size that a particular MTS spans, but also on the typical number of VOI's present over the run of a replication. Calculation times tend to grow quite a bit when evaluating potential future scenarios that experience an increase of VOI's.

Please observe that Fig. 2A displays a time-series plot of the exposure (i.e. the average number of scenarios generated per hour) of VOI's over a 96 hour simulation period. Hence, one observes that exposure (of which risk is a function) changes over time and thus oil spill system risk as it emerges from moving vessel traffic is a dynamically changing quantity

over time. Thus, to arrive at an overall measure of baseline system risk (2) for an MTS, one aggregates scenario oil outflow risk over an extended simulation period for the entire MTS geographic study area. To arrive at a deeper understanding of the baseline risk described by (1), however, we have developed a graphical format that overlays the distribution of scenario risks in (1) across a nautical map using a color scale. This geographic profile format to display oil spill risk across an MTS is described in more detail in Sect. 6.

Risk intervention MTS simulation cases, indicated as the blockers of the causal path ways in Fig. 1, are implemented as modifications of the base case MTS simulation scenario. Risk intervention effectiveness evaluation next involves a comparison of the aggregated system wide risk evaluations over the entire MTS's study area. Separate geographic risk profiles for each case serve to further explain potential changes in risk distribution across an MTS's study area from one risk intervention case to another. We shall use Sects. 3, 4, and 5 to highlight some recent advances made to our maritime risk simulation methodology above for the generation of triplets (s_i, l_i, c_i) in (1), respectively. Section 7 details a sample effectiveness analysis of the three intervention measures depicted in Fig. 1 in the geographic context of the Puget Sound and surrounding waters.

3 Advances in simulation construction of an MTS

In this section, we shall describe some recent improvements to arrive at a more detailed simulation of an MTS. The first two sub sections deal with providing a higher level of detail in simulating the travel patterns and the maritime environment. The third subsection deals with an enhanced recording process to generate grounding accident scenarios.

3.1 Using AIS and radar data in route development

Automatic independent surveillance (AIS) has been used for quite some time in aviation, but its use is becoming more prevalent as a navigational tool on board of vessels as well. At set intervals, it automatically transmits the position of the vessel along with a time stamp and vessel id to an AIS data repository. Hence, already available radar data is more frequently supplemented with AIS data and may replace the need for radar data altogether in the near future. However, as with any data recording process, raw data, be it radar or AIS, has errors within it that either occur at the transmission end or at the receiving end. Figure 4A plots an example plot of automatically collected raw AIS and radar data. Observe that some routes travel over land which is impossible. Figure 4B details a plot of vessel routes after a data cleansing analysis process. Below, we shall describe some of the automated "data-cleansing" algorithms that were used to construct the 1834 vessel routes depicted in Fig. 4B from Fig. 4A. Utilizing these algorithms, a cleansed system of vessel routes was constructed and used in a one year simulation for the MTS analysis in Sects. 6 and 7. Vessels arrive to the MTS according to their original arrival time and location and follow a "cleansed" route to its destination. Without a doubt, the availability of AIS data allows one to construct a more accurate traffic pattern across an MTS as compared to radar data on its own.

Let $\{(x_1, y_1), \ldots, (x_n, y_n)\}$ denote a series of longitude and latitude coordinates obtained from a way point data repository that defines a recorded transit. Each transit may include thousands of points. The computational effort required to calculate movements of vessels in the simulation increases with the number of points n along a route. Hence, we must attempt to keep n per transit as low as possible while maintaining a reasonable curvature of vessel routes along the waterways. The first cleaning step removes points when the vessel is

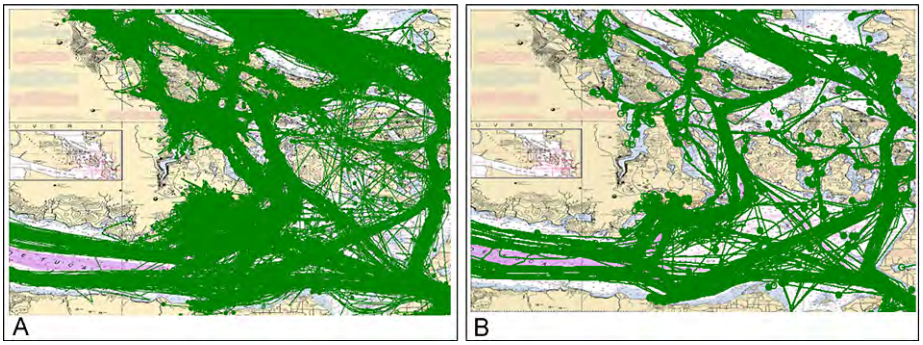

Fig. 4 (**A**) Raw AIS + Radar data; (**B**) Cleaned vessel routes as simulation input

stationary. We consider each pair of successive points. If the j-th point and $(j+1)$-th point are the same, we remove the latter one.

The second cleaning step removes points along a straight line. We consider each sequence of three successive points, (x_{j-1}, y_{j-1}), (x_j, y_j) and (x_{j+1}, y_{j+1}) for $j = 2, \ldots, n-1$. If the middle point (x_j, y_j) lies on the line between the outer ones, one can obviously remove it. However, even if it does not lie exactly on the line, a small deviation might not affect curvature to a great extent. Thus, we calculate the perpendicular distance h between the middle point (x_j, y_j) and the line between (x_{j-1}, y_{j-1}) and (x_{j+1}, y_{j+1}) given by

$$h = d_{j-1,j}^2 - \frac{d_{j-1,j}^2 - d_{j,j+1}^2 + d_{j-1,j+1}^2}{4d_{j-1,j+1}^2}, \tag{3}$$

where d_{kl} is the distance between the k-th and l-th point along the transit route. If h is less than a pre-described threshold ϵ, the midpoint is removed. Selection of ϵ depends on a trade-off between maintaining route curvature and a reduction in the number of points. In Fig. 2, scenario counts are aggregated in a grid of $\frac{1}{2} \times \frac{1}{2}$ nautical miles and are displayed dynamically using a color scale during an animation of the MTS simulation. Hence, the threshold ϵ in that case ought to be less than $\frac{1}{2}$ nautical miles. For the analysis in Sects. 6 and 7, an iterative process was followed starting with $\epsilon = 0.001$ nautical miles per route. If a "cleansed" route resulted in more than 1000 points, a second pass was made using $\epsilon = 0.01$ nautical miles, etc. A threshold of a 1000 points was selected since it visually preserved curvature for even the longest route. Using this process ϵ never exceeded 0.01 nautical miles. Test runs of the MTS simulation with routes of less than 1000 points also resulted in manageable calculation times. Recall, a full year simulation to generate a base case database of accident scenarios for the evaluation of (1) in Sect. 6 required about 15 hours of run time on a Sun Ultra workstation with a 64 bit operating system.

The third cleaning step involves removing recording errors or location sensing errors. Some transit routes exhibit long straight lines with some passing over land (see Fig. 4A). This appears to be an error within the way point data collection and transmission process. Transmission errors either default to the location of an on-shore signal collection device or to the location of the AIS data repository. The most commonly observed way point collection error involved the $(j-1)$-th and $(j+1)$-th points being accurately recorded, but the j-th point being erroneous. To remove these points, an upper bound δ on the distance that a vessel could transit in the time between recording $d_{j,j+1}$ is considered. Utilizing this upper bound, and considering successive three points, if both $d_{j-1,j} > \delta$ and $d_{j,j+1} > \delta$, the j-th point

was removed. Since vessel location recording times vary between 15 seconds and every 2 minutes and since no vessel can travel faster than 50 knots per hours, this third step cleansing process can be started with a threshold distance of $\delta = \frac{2}{60} \times 50 = 1\frac{2}{3}$ nautical miles. Using an iterative process, a value $\delta = 5$ resulted in the removal of these transmission errors for the analysis in Sect. 6.

Each of the three cleansing steps above resulted in a reduction of the number of points of each transit route enhancing computational efficiency. While most of the recording errors were removed using the three approaches, some unfortunately remained, and a final visual evaluation of all corrected transit routes involved an additional manual cleansing process. The MTS simulation program was augmented to plot each route on the nautical chart to allow for the manual removal of remaining erroneous points. This process led to, for example, the 1834 vessel routes plotted in Fig. 4B. Observe from Fig. 4B that a few vessel routes in the center top of this chart still pass over land. However, no VOI's for the analysis example in Sects. 6 and 7 transit near this area and a point of diminishing returns was reached.

3.2 Simulating currents

Environmental variables such as wind, visibility, and current affect the likelihood l_i of accident scenarios s_i in (1). Hourly wind data can be downloaded from the national climatic data center (NCDC 2007) for weather stations within a geographic area and be replayed directly in the MTS simulation. Hourly land visibility can typically be downloaded from area airports. Sea visibility or sea fog data on the other hand is not collected electronically, nor are hourly current observations. Merrick et al. (2003) describes an hourly sea visibility model augmenting land visibility data. It is constructed using hourly dew point and water temperature data as inputs. Both may typically be downloaded from the national climatic data center (NCDC 2007) as well.

To model current behavior across the MTS study area, electronic current tables were constructed for 130 current stations to support the analysis in Sects. 6 and 7. Information from a variety of data sources was reconciled with one another to construct these current tables. The primary data sources were the WXTIDE32 (2007) software by Michael Hopper, the NOAA (2007) tides and current web-site and the MAPTECH (2007) software. Both the WXTIDE32 (2007) and MAPTECH software are used by mariners on the water to make operational decisions. The WXTIDE32 (2007) software provides an ASCII format of current station tables allowing for a straightforward database format conversion. Figure 5 illustrates the geographic distribution of some current stations across the San Juan Islands in Washington State. Observe that the timing of ebb, slack and flood differs from current station to current station since some are in their ebb state (blue), while others are in their flood state (red). The length of a line segment during the MTS simulation is reflective of the current strength (in knots). Below we shall describe the modeling procedure in more detail.

The information sources above provide current tables for the current stations within a geographic area. Some of these are referred to as the so-called "current reference stations". Current tables for other stations are in fact derived in these information sources from the current reference stations using current modifier variables (also provided by these sources). Hence, to model currents in an MTS simulation, one only needs to construct electronic current tables for the reference stations, in our case: Admiralty Inlet, Deceptions Pass, Gray Harbor, Rosario Strait, San Juan Channel South Entrance, Strait of Juan de Fuca and The Narrows End. Figure 6A provides a snapshot view of a section of an WXTIDE32 (2007) ASCII current table for the reference station Rosario Strait. Figure 6B gives a snapshot of additional current station info and current modifier parameters. The columns FD and ED

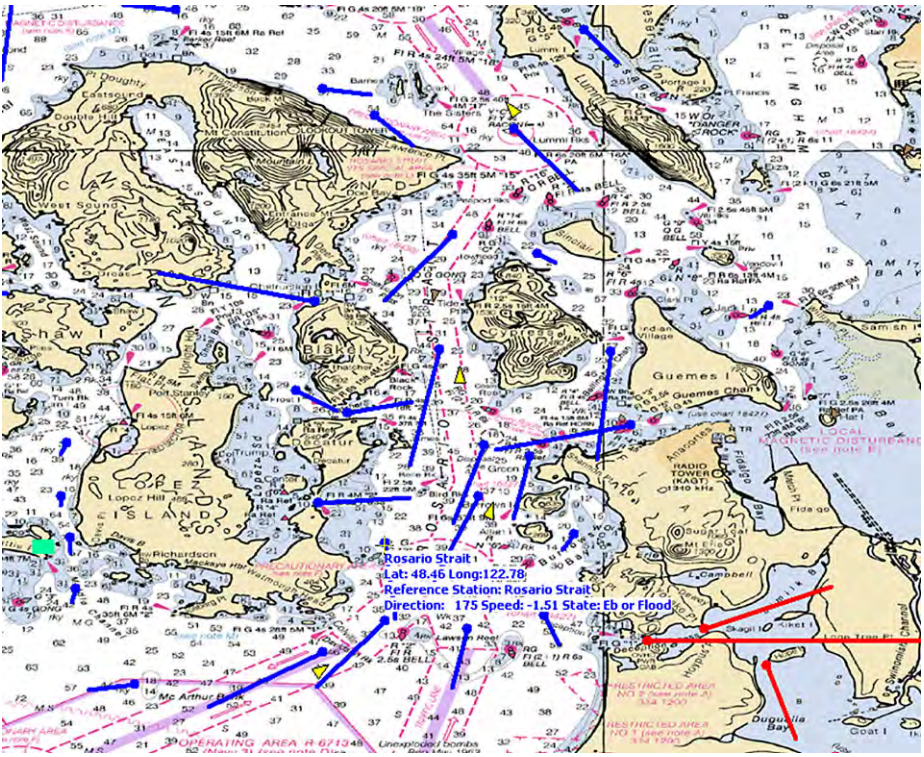

Fig. 5 Geographic locations of some current stations in an MTS study area

provide the current direction for a station at flood and ebb. To derive the current strength at flood state for the non-reference station "Admiralty Head" (Row 1 in Fig. 6B) one multiplies the current strength of its reference station (indicated by the column RS) "Admiralty Inlet" (Row 2 in Fig. 6B) using the high tide multiplier (HTM) 1.29 and one delays (because of the "+" in column HTTM) its max flood state by 0 hours (Column HTHM) and 3 minutes (Column HTMM). Low tides at non-reference stations may be evaluated in a similar manner using the columns starting with "LT".

Finally, current tables only specify when a current station's high tide, low tide, and slack states are occurring (see Fig. 6A) and provide the max current speeds at these times. To model the current in between the max ebb and max flood stages, a harmonic curve may be fitted in between. Figure 7 provides a section of a resulting fitted time series for the current reference station Rosario Strait displayed in Fig. 5. The current experienced by a particular vessel within the MTS simulation was determined as that of its closest current station within the MTS study area.

3.3 Generating collision and grounding scenarios

The primary purpose of the MTS simulation is to generate potential accident scenarios to arrive at a deeper understanding of baseline system risk (1). Accident scenario databases (see Fig. 2B) are constructed for collision and groundings, separately. Moreover, a further separation of the grounding database is implemented to distinguish those groundings pre-

```
Rosario Strait, Washington Current
Units are knots, initial timezone is PST
January 2005 low is -3.5kt, high is 2.7kt, range is 6.2kt.
Predicted historical low is -4.8kt, high is 4.0kt, range is 8.8kt.

Sunday      Monday      Tuesday     Wednesday   Thursday    Friday      Saturday

Full 12-26     12-27       12-28       12-29       12-30       12-31       01-01
F0314  2.0 S0032 -0.0 S0105  0.0 S0137  0.0 S0208  0.0 S0240  0.0 S0310  0.0
S0725 -0.0 F0338  2.1 F0404  2.1 F0435  2.2 F0510  2.1 F0547  2.1 F0621  1.9
E0954 -1.0 S0757 -0.0 S0826 -0.0 S0852 -0.0 S0916 -0.0 S0938 -0.0 S0952 -0.0
S1256  0.0 E1023 -1.1 E1056 -1.2 E1132 -1.2 E1213 -1.3 E1257 -1.4 E1338 -1.5
F1347  0.2 S1352  0.0 S1501  0.0 F1605 -0.1 F1657 -0.1 F1747 -0.1 F1839 -0.0
S1443 -0.0 F1431  0.1 F1516  0.0 E2217 -2.5 E2239 -2.2 E2303 -1.9 E2338 -1.5
E2047 -2.9 S1510 -0.0 S1532 -0.0           E2121 -2.8 E2151 -2.7

   01-02    LQtr 01-03     01-04       01-05       01-06       01-07       01-08
S0344  0.0 E0030 -1.0 E0238 -0.6 S0137 -0.0 S0347 -0.0 F0024  1.5 F0109  1.9
F0658  1.7 S0420  0.0 S0459  0.0 E0404 -0.3 E0520 -0.3 S0504 -0.0 S0556 -0.0
S1007 -0.0 F0736  1.4 F0818  1.1 S0548  0.0 S0703  0.0 E0638 -0.3 E0753 -0.5
E1421 -1.7 S1020 -0.0 S1035 -0.0 F0905  0.7 F1001  0.5 S0922  0.0 S1040  0.0
S1857  0.0 E1502 -2.0 E1541 -2.2 S1059 -0.0 S1132 -0.0 F1101  0.4 F1158  0.3
F1933  0.1 S1931  0.0 S2009  0.0 E1621 -2.5 E1705 -2.8 S1215 -0.0 S1306 -0.0
S2011 -0.0 F2033  0.3 F2145  0.5 S2049  0.0 S2131  0.0 E1754 -3.0 E1848 -3.2
           S2200 -0.0           F2314  1.0           S2213  0.0 S2255  0.0
```

(A)

ID	Name	Lat	Long	RS#	FD	ED	HTTM	HTHM	HTMM	HTM	LTTM	LTHM	LTMM	LTM
1	Admiralty Head	48.1500	122.7000	2	127	7	+	0	03	1.29		0	07	1.2
2	Admiralty Inlet	48.0333	122.6333	2	161	345	+	0	00	1		0	00	1
3	Agate Pass 1	47.7167	122.5500	2	0	0	–	1	00	0.8		0	59	0.69
4	Agate Pass 2	47.7128	122.5655	2	198	19	+	0	53	2		0	47	1.39
5	Alden Point	48.7578	122.9803	107	7	167	+	0	26	0.89		0	53	1.1
6	Alki Point	47.5755	122.4280	2	142	312	+	0	44	0.3		0	39	0.2
7	Apple Cove Point	47.8167	122.4667	2	150	350	+	0	11	0.3		0	29	0.3
8	Balch Passage	47.1875	122.6972	126	278	89	–	1	07	0.4		0	40	0.8
9	Barnes Island	48.6858	122.7888	107	297	122	+	1	20	0.6		0	08	0.5
10	Bellingham Channel	48.5603	122.6637	107	27	167	–	0	08	1.1		0	51	1.2

(B)

Fig. 6 (**A**) Example section of an ASCII current table generated by the WXTIDE32 software. (**B**) Current parameters to evaluate currents at non-reference stations

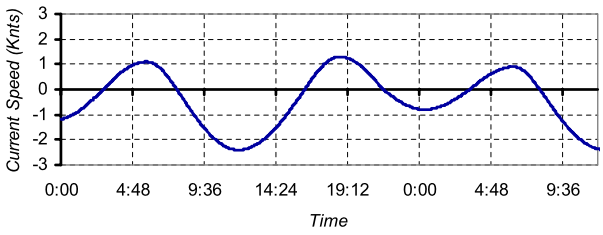

Fig. 7 Example current speed for the Rosario Strait current station over time

ceded by a propulsion or steering failure (drift groundings) from those that are preceded by a human error, navigational aid or nearby vessel failure (powered groundings).

To capture potential collision accident scenarios, any pairwise interaction between a VOI and an IV was recorded within a distance that the VOI can travel within 5 minutes. Thus, e.g., 12 knots was converted to a one nautical mile radius. In Merrick et al. (2000, 2003) and van Dorp et al. (2001) this distance was held constant regardless of the VOI's speed. The

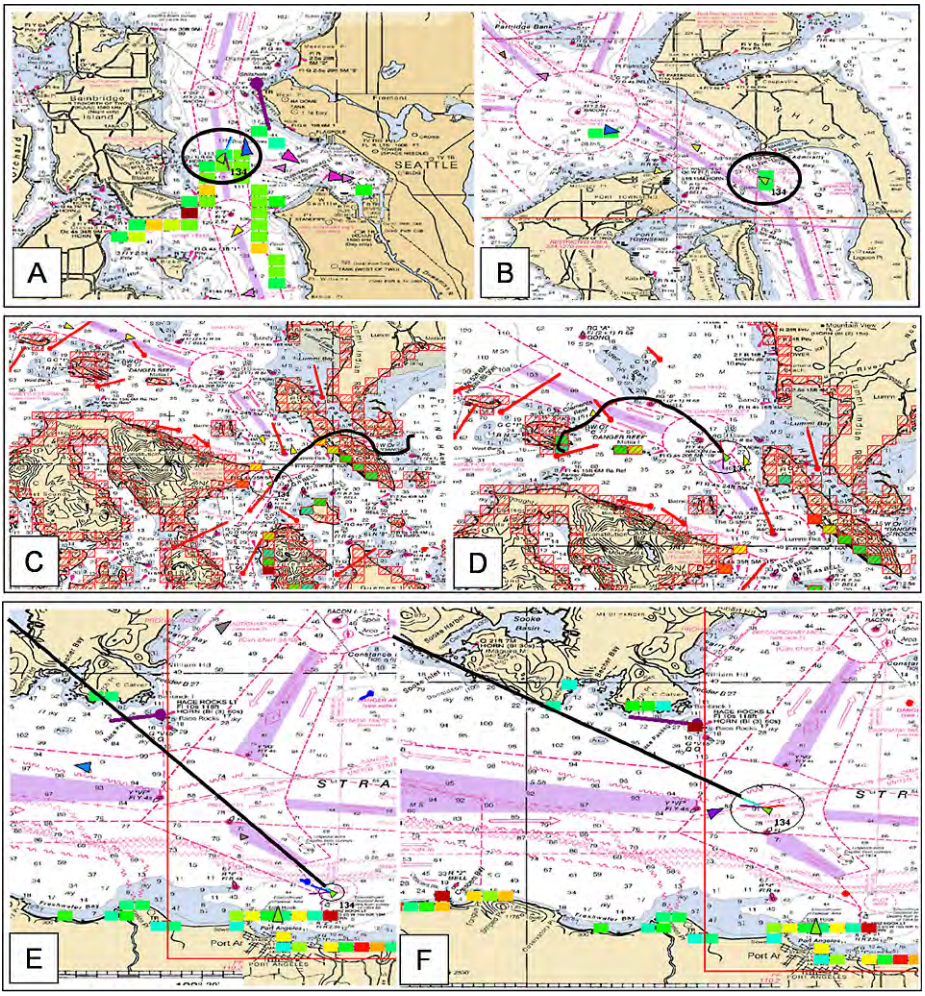

Fig. 8 Recording potential accident scenarios. (**A**–**B**) collisions; (**C**–**D**) drift groundings; (**E**–**F**) powered groundings

left snapshot of the MTS maritime simulation in Fig. 8A demonstrates an interacting vessel in VOI's 134 "counting zone". The counting color scheme changes dynamically, assigning darker colors to those grid cells with a higher number of potential collision scenarios. Observe from Fig. 8B that a collision scenario is recorded for an IV that is not within the immediate "counting zone" of the VOI. This could happen when the future crossing point of the IV is within a certain threshold distance from the front or the back of the VOI and that crossing would occur within a threshold time. Such a counting procedure is reminiscent of a future Closest Point Approach (CPA) evaluation used when actually navigating vessels. To mimic this approach the threshold distance and threshold time were set to 1.5 nautical miles and 20 minutes, respectively.

In Merrick et al. (2000, 2002) grounding accident locations where analyzed as a function of the location of the potential incident occurring. Calculation power at the time prevented on-the-fly drifting path evaluations and a separate vessel drift simulator was developed (Mer-

rick 2002) to evaluate potential shore locations of grounding accidents. The procedure for generating grounding accident scenarios was enhanced to evaluate potential shore locations on-the-fly, and to support the analysis in Sects. 6 and 7. Potential drift or power grounding locations were evaluated using a shore line definition consisting of shoreline grid cells also of $\frac{1}{2} \times \frac{1}{2}$ nautical miles. Potential locations of drift grounding accident scenarios were recorded by predicting the drifting path of a tanker five hours out. This drifting path takes into account future wind speeds, currents and slows the tanker down over the time it is drifting. This path follows the drift model of the NOAA (1997) publication also implemented in Merrick (2002). A drift grounding accident scenario is recorded for the first grid cell that falls on the drifting path and is part of the shore line definition. Figures 8C and 8D show a drifting path of a VOI as well as the grid cells of the shore line definition. Observe from Figs. 8C and 8D that a drift accident scenario is recorded where this drifting path intersects the shore line definition for the first time.

To count potential accident scenario locations at the shore line for powered groundings, a straight line following the direction of the VOI is projected. The assumption here being that those shoreline grid cells that have more frequently a VOI coming directly towards them will also have a higher powered grounding risk. These straight line projections are drawn for a distance that the VOI can travel five hours out (assuming a constant speed over that time frame). The first grid cell of the shoreline definition that intersects this straight line projection will be recorded as a potential power grounding accident scenario for the evaluation of baseline risk (1). The two snapshots in Figs. 8E and 8F illustrate this procedure for powered groundings.

4 Advances in accident frequency analysis of collisions and groundings

The context of the oil spill risk analysis presented in this paper was an oil spill risk assessment conducted from 2006–2008. A comprehensive accident data collection process (see the third oval in the causal chain in Fig. 1) recorded one collision and one grounding over an 11 year period. A naive approach towards evaluating the likelihoods l_i in (1) would distribute the annual accident frequency evenly across the MTS generated accident scenarios. This approach may be considered naive since accident likelihoods differ from scenario to scenario, but not enough data exists to allow for a differentiation via a classical statistical means. Hence, we rely on expert judgment to elicit relative likelihoods for a series of paired comparison questions to estimate the effect of multiple accident scenario descriptors such as IV type, traffic scenario, wind, visibility, and current etc., on the accident likelihood l_i.

The inference procedure is described in detail in Merrick et al. (2005) and Szwed et al. (2006). A total of 9 questionnaires were developed that were distributed to 38 experts over 7 separate elicitation sessions dispersed over a one year period. The combined number of years of sailing experience of the experts who participated in the elicitation process exceeded 922. A single expert participating in a full set of questionnaires would have contributed over 10 hours of elicitation time spread over multiple elicitation sessions. The maritime experts who participated in this study donated their time solely for the enhancement of maritime safety levels and did not benefit personally from elicitation participation. In this section, we shall review the elicitation of relative collision likelihoods using an enhanced questionnaire format to reduce overall elicitation time. This section also serves as prelude to a novel grounding accident probability model that now includes a time-to-shore variable that is recorded during the accident scenario recording process (described in Sects. 2 and 3.3). Needless to say, longer times-to-shore result in lower grounding accident likelihoods. In fact,

Situation 1	TANKER DESCRIPTION	Situation 2
Strait of Juan de Fuca East	Location	-
Inbound	Direction	-
Laden	Cargo	-
1 Escort	Escorts	-
Untethered	Tethering	-
	INTERACTING VESSEL	
Shallow Draft Pass. Vessel	Vessel Type	-
Crossing the Bow	Traffic Scenario	-
Less than 1 mile	Traffic Proximity	-
	WATERWAY CONDITIONS	
More than 0.5 mile Visibility	Visibility	-
Along Vessel	Wind Direction	-
Less than 10 knots	Wind Speed	25 knots
Almost Slack	Current	-
Direction	Current Direction	-

Complete Propulsion Loss		
More? : ____	9 8 7 6 5 4 3 2 1 2 3 4 5 6 7 8 9	____ : More?
Situation 1 is worse	<==========X==========	Situation 2 is worse

Complete Steering Loss at a Moderate Angle		
More? : ____	9 8 7 6 5 4 3 2 1 2 3 4 5 6 7 8 9	____ : More?
Situation 1 is worse	<==========X==========	Situation 2 is worse

Complete Navigational Aid Loss		
More? : ____	9 8 7 6 5 4 3 2 1 2 3 4 5 6 7 8 9	____ : More?
Situation 1 is worse	<==========X==========	Situation 2 is worse

Human Error		
More? : ____	9 8 7 6 5 4 3 2 1 2 3 4 5 6 7 8 9	____ : More?
Situation 1 is worse	<==========X==========	Situation 2 is worse

Nearby Vessel Incident (but you do not know the specifics)		
More? : ____	9 8 7 6 5 4 3 2 1 2 3 4 5 6 7 8 9	____ : More?
Situation 1 is worse	<==========X==========	Situation 2 is worse

Fig. 9 Example question of a paired comparison questionnaire of situations for tanker collision accident attribute parameter assessment given all incidents

tanker paths (described in Sect. 3.3) were only projected 5 hours out since it was judged unlikely during this study that longer times could result in a grounding due to available external vigilance offered not only by the USCG VTS, but also other vessel traffic.

4.1 Enhancements in the collision elicitation process

The accident probability models in Merrick et al. (2005) and Szwed et al. (2006) follow the set-up:

$$\Pr(\mathit{Collision}|\mathit{Incident},\ \underline{X}) = P_0 \exp\left\{\underline{\beta}^T \underline{X}\right\}, \tag{4}$$

where $\underline{X}$ is a normalized vector constructed from accident scenario descriptors exemplified by the record definition in Fig. 2B. Each element of the vector $\underline{X}$ is normalized to a $[0, 1]$ scale to allow for a comparison of elements of the parameter vector $\underline{\beta}$ in terms of their effect on l_i in (1). A vector of all ones $\underline{X} = \underline{1}$ describes the worst case accident scenario and a vector of all zeros $\underline{X} = \underline{0}$ describes the best case accident scenario. Figure 9 shows the format of a question to elicit relative likelihoods of an accident probability questionnaire

consisting of 44 questions. Each question describes two situations only differing in a single attribute. An expert is asked to compare how much more likely an accident is to occur given the occurrence of an incident in each of these two situations. The expert's answer would give us, for a particular comparison of Situations 1 and 2, the value of:

$$\frac{\Pr(Collision|Incident, \underline{X}_1)}{\Pr(Collision|Incident, \underline{X}_2)} = \exp\left\{\underline{\beta}^T[\underline{X}_1 - \underline{X}_2]\right\}. \tag{5}$$

Taking natural logarithms on both sides of (5) yields

$$\ln\left[\frac{\Pr(Collision|Incident, \underline{X}_1)}{\Pr(Collision|Incident, \underline{X}_2)}\right] = \underline{\beta}^T[\underline{X}_1 - \underline{X}_2]. \tag{6}$$

The logarithms of expert responses (6) serve as data for a Bayesian inference procedure described in Merrick et al. (2005) and Szwed et al. (2006) to estimate the parameters $\underline{\beta}$ in (4). The parameter P_0 is used to calibrate the overall predicted collisions frequency by the MTS to be consistent with the observed collision frequency of 1 per 11 years.

The questionnaire of 44 questions of the format in Fig. 9, was further subdivided in three parts. During Questions 1 through 18 the "Tanker Description" in Fig. 9 varied from Situation 1 to Situation 2 in a single attribute, whereas the description of the "Interacting Vessel" and the "Waterway Conditions" were held constant. During Questions 19 through 29 the "Interacting Vessel" varied from Situation 1 to Situation 2 in a single attribute, whereas the "Tanker Description" and the "Waterway Conditions" were held constant. Finally, during Questions 30 through 44 the "Waterway Conditions" varied from Situation 1 to Situation 2 in a single attribute, whereas the "Tanker Description" and the "Interacting Vessel" were held constant. A first questionnaire was provided with only the propulsion failure as the described incident preceding the accident allowing the expert to concentrate purely on the situational descriptions of these 44 questions. Next, experts were asked to record their answers of this first questionnaire in a second questionnaire with the extended question format of Fig. 9 (i.e. including answer scales for the other incidents). In a second pass through these 44 questions, the expert were asked to compare the two comparisons from the perspectives of the other incidents: steering failure, navigational aid failure, human error or nearby vessel failure that could have preceded the accident. This second pass provided experts with the benefit of having their answers of the first pass fostering consistency in the overall expert responses while experts were able to focus on the differences that the various incidents may have when comparing the two situations.

The two-pass questionnaire process above with a three-section subdivision of a questionnaire is an enhancement of our prior elicitation processes primarily to reduce overall elicitation time. Experts were able to respond to the questionnaires above over two elicitation session lasting about two hours each. Elicitation sessions were spread out over two days. The enhanced efficiency above was paramount since participation in the expert judgment elicitation was purely voluntary, involving no renumeration for the experts, and proved to be limited. The increased efficiency comes at a price from an inference point of view however. While interactions between accident descriptors may be estimated within the three groups "Tanker Description", "Interacting Vessel", and "Waterway Conditions", no interactions can be estimated between accident descriptors across these groups.

4.2 Accommodating a time-to-shore variable in a grounding accident probability model

Both the drift grounding and powered grounding accident scenario recording process, described in Sect. 3.3, store the value of a time-to-shore variable t as an accident descriptor to

the base case database of scenarios for the evaluation of (1). Longer times-to-shore have a depressing effect on a grounding likelihood. A grounding accident probability model reminiscent of (4) was developed that includes t while allowing for the estimation of accident likelihood parameters via the same paired comparison relative likelihood elicitation procedure for the evaluation of baseline risk (2). Its expression is given by:

$$\Pr(\mathit{Grounding}|\mathit{Incident}, \underline{X}, t) = P_0 \exp\Big\{-\alpha_0 t\Big\} \exp\Big\{-\alpha_0 \underline{\gamma}^T (\underline{1} - \underline{X}) t\Big\}, \tag{7}$$

where $\underline{1}$ is a vector with elements equal to 1. Recalling that each element of the vector $\underline{X}$ is normalized to a $[0, 1]$ scale, one immediately observes that (7) decreases with increasing t provided $\alpha_0 > 0$ and $\underline{\gamma} > 0$. Pre-specifying the time-to-shore variable t_q in a paired comparison question similar to Fig. 9, one obtains from (7)

$$\frac{\Pr(\mathit{Grounding}|\mathit{Incident}, \underline{X}_1, t_q)}{\Pr(\mathit{Grounding}|\mathit{Incident}, \underline{X}_2, t_q)} = \frac{\exp\{-\alpha_0 \underline{\gamma}^T (\underline{1} - \underline{X}_1) t_q\}}{\exp\{-\alpha_0 \underline{\gamma}^T (\underline{1} - \underline{X}_2) t_q\}}. \tag{8}$$

Taking natural logarithms on both sided of (8) yields

$$\ln\left[\frac{\Pr(\mathit{Grounding}|\mathit{Incident}, \underline{X}_1, t_q)}{\Pr(\mathit{Grounding}|\mathit{Incident}, \underline{X}_2, t_q)}\right] = \{\alpha_0 t_q \underline{\gamma}\}^T [\underline{X}_1 - \underline{X}_2]. \tag{9}$$

When experts were asked informally (after the collision elicitation session described in Sect. 4.1) if their answers to the paired comparison scenarios would change substantially if the accident scenario would have changed from a collision to a grounding, their answer was that they would not. This suggests a further substitution of

$$\underline{\beta} = \{\alpha_0 t_q \underline{\gamma}\}^T \tag{10}$$

into (7). The right hand side (RHS) of expression (9) in that case reduces to the RHS of (6) and expression (7) to:

$$\Pr(\mathit{Grounding}|\mathit{Incident}, \underline{X}, t) = P_0 \exp\Big\{-\alpha_0 t\Big\} \exp\Big\{-\underline{\beta}^T (\underline{1} - \underline{X}) \frac{t}{t_q}\Big\}. \tag{11}$$

Hence, it may be deduced that the expert judgment elicitation burden may be once more significantly reduced, provided the MTS simulation is separately calibrated to an observed grounding accident frequency per year using α_0, t_q and P_0 in (11) as calibration constants.

Since experts judgment participation for the analysis in Sects. 6 and 7 was voluntary (and did not involve renumeration for the experts) it proved to be limited and the approach involving expressions (10) and (11) was followed. Setting $\alpha_0 = \ln(2)$ implies a 50-50 save probability of a distressed tanker in a worst state environment $\underline{X} = \underline{1}$ (implying e.g. high winds, high currents, low visibility, etc.) in each additional hour to respond. Without additional information this appears to be a reasonable assumption. Next, calibrating the MTS base case analysis in Sect. 6 to be consistent with one observed grounding accident per 11 years and a ratio of 3 to 1 of groundings preceded by human error to mechanical failures, resulted in a calibration value of $t_q = 0.834$, and a calibration value of $P_0 \approx 0.528$ in (11) for the incident type "Human Error" and a calibration value $P_0 \approx 0.405$ given the incident types "Steering Failure", "Propulsion Failure". An overall ratio of 3 to 1 of human error to mechanical failures was observed in the historical accident/incident analysis. Utilizing (10)

Table 1 Probabilities of grounding given an incident failure in the least risk state ($\underline{X} = 0$) and most risk state ($\underline{X} = 1$) and a time to shore of 5 hours

Best State ($\underline{X} = 0$)	Tankers	Tugs	Worst State ($\underline{X} = \underline{1}$)	Tankers	Tugs
Propulsion Failure	9.729E-41	5.991 E-51	Propulsion Failure	0.0127	0.0127
Steering Failure	5.894E-53	2.756E-51	Steering Failure	0.0127	0.0127
Nav. Aid Failure	8.714E-32	6.011E-35	Nav. Aid Failure	0.0127	0.0127
Human Error	3.819E-47	9.576E-50	Human Error	0.0165	0.0165

and (11) we have from $\alpha_0 = \ln(2)$ and a five hour of available response time in the worst state ($\underline{X} = 1$):

$$\Pr(\textit{Grounding}|\textit{Incident}, \underline{X} = \underline{1}, t = 5) = P_0\left(\frac{1}{2}\right)^5 = \frac{P_0}{32} \tag{12}$$

and in the least risky state ($\underline{X} = 0$):

$$\Pr(\textit{Grounding}|\textit{Incident}, \underline{X} = \underline{0}, t = 5) = P_0\left(\frac{1}{2}\right)^5 \exp\left\{-\left[\sum_{i=1}^{n} \beta_i\right]\frac{5}{t_q}\right\}. \tag{13}$$

Recall that potential tanker paths for grounding scenarios were only drawn five hours out since it was deemed extremely unlikely a grounding would occur due to available external vigilance in the Puget Sound study area. Further substitution of $t_q = 0.834$ and the calibration values for P_0 above in (12) and (13) yielded the values in Table 1 for grounding probabilities by incident type, separated by tankers and tugs and the best state ($\underline{X} = 0$) and worst state ($\underline{X} = 1$), given a five hour "time-to-shore" variable t. Please observe that the information in Table 1 appears to be reasonably consistent with the grounding accident scenario recording procedure in Sect. 3 to predict a tanker paths only for 5 hours out.

5 Accounting for vessel fuel losses in oil outflow modeling

The Transportation Research Board (TRB) from the National Academies of Sciences (NRC 2001) concluded in 2001 that a descriptive oil outflow model was needed to evaluate the differences in tanker design performance of single hull and double hull tankers in collisions and grounding accidents. The primary reason for arriving at this conclusion was a lack of data of double hull tanker accidents. Only one hundred historical collision and grounding accidents were recorded during the period 1980–1990 which involved only single hull tankers. Probability density functions (pdf) were created by IMO (1995) from this data set for longitudinal and transversal damage extents, but neither pdf's were able to take into account the specifics of a particular accident scenario such as vessel sizes, vessel speeds and their interaction angle. The TRB commissioned a study which resulted in the SR259 report (NRC 2001). A total of 80,000 physical simulation accident scenarios were conducted during this study linking input parameters such as point of impact, vessel mass, vessel speed and vessel compartments to oil outflow values.

Each physical simulation scenario in this TRB study was computationally intensive by itself. This computational complexity prohibits the direct integration of these physical damage simulations with a MTS simulation approach. However, via a statistical analysis of these

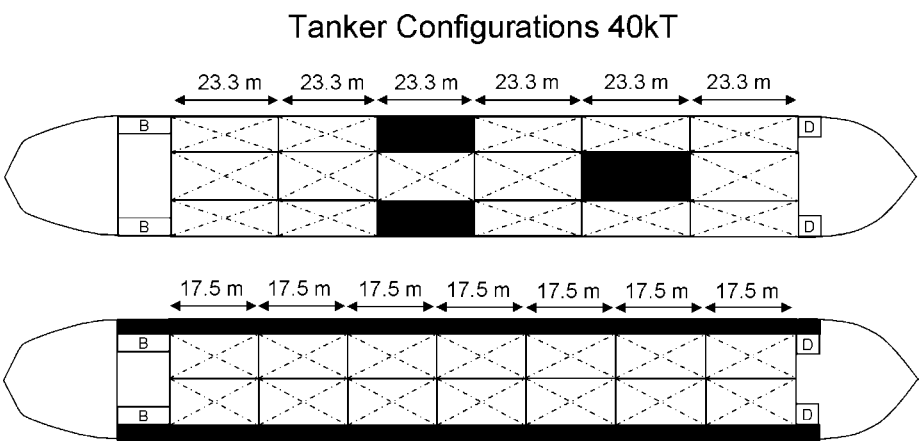

Fig. 10 Worst case assumption locations for bunker fuel tanks (*B*) and diesel fuel tanks (*D*) for tankers. Figure is modified from SR259 Report

80,000 physical simulation accident scenarios, an explicit oil outflow model was developed linking the input parameters from this TRB study to scenario output longitudinal and transversal damage extents, and nevertheless adheres to the same kinetic energy principles. The impact location and damage extent parameters of this model determine what compartments in a tank vessels configurations are penetrated. The construction of this oil outflow model is described in more detail by van van de Wiel (2008) and is the topic of a separate paper (van de Wiel and van Dorp 2009). All cargo or fuel from a penetrated tank is assumed lost. Figure 10 depicts typical tanker compartments of a 40kt single hull and a 40kt double hull tanker.

The collision of a container vessel (the Cosco Buscan) with a pillar of the San Francisco Bay bridge in 2007, and its subsequent vessel fuel losses, triggered the largest US oil spill in San Francisco Bay in more than a decade (USCG 2008). Hence, the oil outflow model described in van de Wiel and van Dorp (2009) also allows for an evaluation of vessel fuel loss in addition to cargo spills of crude and petroleum products using a vessel's compartment design. To be able to accommodate diesel fuel and bunker fuel oil outflow calculations, Fig. 10 was augmented from its version in the SR259 report (NRC 2001) with the displayed bunker fuel and diesel fuel compartments in Fig. 10. While certainly there can be more than two bunker fuel tanks and two diesel fuel tanks on any given deep draft vessel, the locations in Fig. 10 for these vessel fuel tanks were modeled from a worst case analysis perspective. Bunker fuel compartments were located towards the stern (where the main engine is located) and diesel fuel compartments towards the bow. Note that from Fig. 10 it follows that a double hull tanker is provided the benefit of the double hull for the diesel fuel and bunker fuel compartments as well.

In our oil outflow analysis the oil loss from a struck vessel is weighted by the probability of it being struck given the two vessels involved in a collision scenario. Section 5.1 develops a "vessel struck probability" model. In case the length of the struck vessel is less than or equal to the width of the striking vessel, all diesel fuel on board of the struck vessel is assumed lost. Section 5.2 presents our approach towards vessel fuel capacity modeling. In all other cases, a separate oil outflow analysis was conducted that first evaluates longitudinal and transversal damage extents using the kinetic energy principles as discussed in van de Wiel (2008). For non-tankers, single hull parameters were used to evaluate bunker

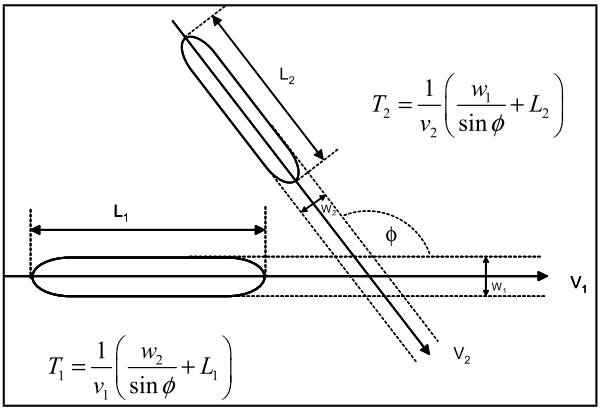

Fig. 11 A schematic of a striking ship-struck ship probability model

and diesel fuel losses. Finally, it was further assumed that no vessel fuel or oil cargo products are lost from the striking vessel.

5.1 Enhancement in struck ship probability model

Potential collision accident scenarios recorded by the MTS simulation for the evaluation of baseline risk (1) contain the description of a VOI and an IV. In the event of two identical vessels crossing each others paths at a 90 degree angle and traveling at exactly the same speeds, a 50-50 chance of either one being the struck or striking vessel is a reasonable assumption. However, this assumption becomes less reasonable when large speed or dimension differentials are present amongst the VOI and IV. Take, for example, an interaction between a tanker and a high speed recreational vessel. Simply from a dimensional perspective it would be more likely that the tanker is hit instead of the recreational vessel. Who strikes and who is struck, has implications with respect to the average oil outflow that one evaluates for such a potential collision accident scenario.

The model below evaluates the probability that either the VOI or the IV is the struck vessel. It utilizes the vessel speeds, the dimensions of both the VOI and IV, and their interaction angle recorded as collision accident scenario descriptors. Figure 11 provides a schematic and geometric explanation of this striking-stuck ship model. Let L_1, w_1, and v_1 be the length, width and traveling speed of the first vessel. Let L_2, w_2, and v_2 be the length, width and traveling speed of the second vessel, and let Φ be the angle of their crossing paths. From these parameters one first evaluates the distance that Vessel 1 is exposed to the potential of a collision, which follows as

$$L_1 + \frac{w_2}{\sin\phi}. \tag{14}$$

From (14) and the speed v_1 one evaluates that Vessel 1's exposure time T_1 to a potential collision is given by:

$$T_1 = \frac{1}{v_1}\left(L_{1+}\frac{w_2}{\sin\phi}\right). \tag{15}$$

Using a symmetry argument one evaluates for the length of time T_2 that Vessel 2 is exposed:

$$T_2 = \frac{1}{v_2}\left(L_{2+}\frac{w_1}{\sin\phi}\right). \tag{16}$$

Next, we set:

$$\Pr(\text{Vessel 1 is struck}) = \frac{T_1}{T_1 + T_2} \quad \text{and} \quad \Pr(\text{Vessel 2 is struck}) = \frac{T_2}{T_1 + T_2}. \tag{17}$$

From expression (17) one evaluates that two identical vessels traveling at the same speed and crossing paths at a 90 degree angles indeed have a 50-50 chance of being the struck vessel. On the other hand, one evaluates from (17), for example, that a tanker with a length 266.3 meters and width of 50 meters, traveling at 8 knots crossing the path of a tug with a length of 34 meters and a width of 12 meters traveling at 12 knots at a $\phi = 135$ degree interaction angle, has approximately an 80% probability of being struck. Thus, in that scenario the tug has approximately a 20% probability of being struck. Oil loss in this collision accident scenario is evaluated as the weighted sum of evaluated oil loss from the tanker and that from the tug with weights 80% and 20%, respectively.

5.2 Estimating bunker and diesel fuel capacities

Vessels in any MTS may range in size and utility from tankers to sailing regattas. The bunker or diesel fuel capacities of these vessels are as diverse as the vessels themselves. In order to include diesel fuel and bunker fuel losses in the oil outflow model, multiple sources were queried. For example, the fuel oil capacities for tankers and tugs are provided in so-called Vessels Particular Questionnaires (VPQ's). These VPQ's detail the fuel oil type and volume capacity of each fuel tank. Bunker and diesel fuel capacities for other deep draft vessels were compiled from various regional and global vessel brokerage firm's web-sites (see, e.g., http://www.ship-technology.com) as well as from ship building publications (see, e.g., Taggart 1980). The data from these sources were compiled to generate the scatter plots for deep draft vessels and tugs in Figs. 12A and B. Please observe from Figs. 12A and B that tugs are shorter than deep draft vessels (at least by a factor of five), but that the maximum value of the y-axis for fuel capacity of deep draft vessels (Fig. 12A) is a factor 10 higher than that of tugs (Fig. 12B).

Regression models were fitted modeling bunker or diesel fuel capacities as a function of the length of a vessel. For deep draft vessels, a power function regression model was fitted for the bunker fuel data and a polynomial regression model for the diesel fuel data in Fig. 12A. Both are plotted in Fig. 12A. Their expressions and R^2 values are given by:

$$\begin{cases} y_{bunker} = 0.256x^{1.76}, & R^2 \approx 78\%, \\ y_{diesel} = 421.456 - 7.931x + 5.460x^2 + (9.861 \times 10^{-5})x^3, & R^2 \approx 24\%, \end{cases} \tag{18}$$

where x is the length of a deep draft vessel. A power function regression was fitted for the diesel fuel data for tugs in Fig. 12B. It is plotted in Fig. 12B. Its expression and R^2 are given by:

$$y_{diesel} = (9.861 \times 10^{-5})x^{4.39}, \quad R^2 = 79\%. \tag{19}$$

Please observe from (18) and (19) that the R^2-values for the bunker fuel of deep draft vessels and diesel fuel of tugs are quite high, whereas the R^2-value for the diesel fuel regression of deep draft vessels should be considered low. Taking into account deep draft vessels lengths, (typically over 102 meters long for the base case oil spill risk analysis in Sect. 6) the relative inaccuracy in deep draft diesel fuel capacity is masked by their larger amount of bunker fuel (which is also heavier then diesel fuels). Utilizing (18) for vessels with a length of more than 102 meters, bunker fuel capacity exceeds diesel fuel capacity by a factor 10 or more.

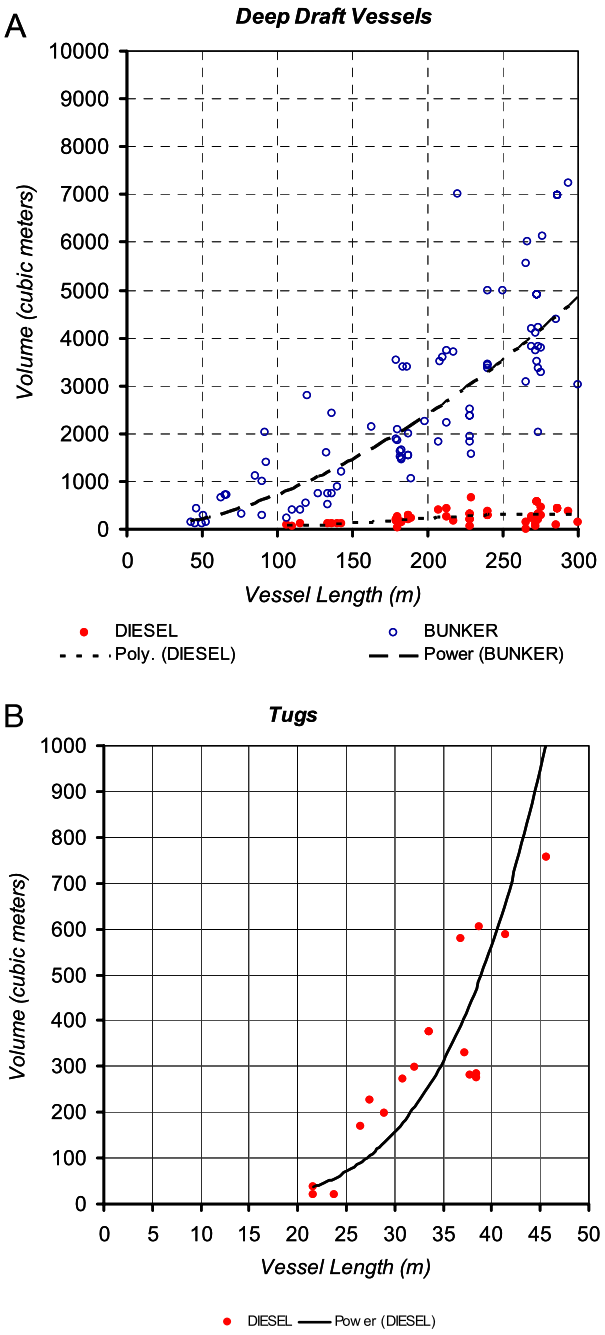

Fig. 12 Scatter plots and least squares regression fits. (**A**) Deep draft vessel bunker and diesel fuel data; (**B**) Tug diesel fuel data

Similar regression equations to those in (18) and (19) were fitted for vessel fuel capacities of other vessel types with R^2-values 75% or higher.

6 Evaluating aggregate baseline risk and describing it in a geographic format

In this section, we shall estimate an aggregate value (2) for baseline oil spill risk (1) using the MTS risk simulation methodology described in this paper. Furthermore, we shall attempt to arrive at a deeper understanding of the set of baseline accident scenarios (1) by developing a graphical format of their geographical distribution of oil spill risk across the MTS study area. The MTS's borders are delineated by the blue line segments in Fig. 13. For a detailed description of this area see for example Evans et al. (2001). VOI's shall be tankers, articulated tug barges, and integrated tug barges which transport both crude oil and refined products in this study area. While the oil spill risk assessment conducted for this study area over 2006–2008 only considered one refinery, we shall consider herein all VOI's that serve the six refineries distributed throughout the study area. Their approximate locations are indicated in Fig. 13. Of Refineries 5 and 6, one has not refined since 1998 and its facilities only serve as a petroleum product tank farm. It shall be assumed for the analysis of baseline risk that all VOI's have double hulls (at the time of the study some of them were still phased in). The northerly route (through Rosario Strait) towards Refineries 1 and 2 is classified as a one way zone for certain larger vessels. An escorting regime for escorting laden tank vessels was implemented in the MTS simulation that mimics the current escorting operations within that study area. Summarizing, our base case scenario is an instance of the causal chain picture in Fig. 1 where all three risk intervention measures have been implemented and are operational.

Aggregate baseline oil spill risk (2) was evaluated in terms of annual average oil losses for four different categories and are provided in cubic meters by accident type in Table 2. The crude cargo and bunker fuel are called persistent oil (PO) since they are "heavier" and less volatile than refined products and diesel fuel. Refined products and diesel fuel shall be referred to as non-persistent oil (NPO). Considering further the VOI or IV origin of the potential oil losses the following four categories are listed in Table 2: VOI PO, VOI NPO, IV PO and IV NPO. The ability of separating oil losses in these categories is a direct result of the advances in oil outflow modeling described in Sect. 5 of this paper. The evaluation of the oil outflows by accident type utilizes the enhancements in our accident frequency models as described in Sect. 3 (as it related to accident scenario generation) and Sect. 4 (as it relates to accident scenario probability modeling). The aggregate results in Table 2 followed from 157,670 generated potential collision scenarios (see Fig. 3) and 1,236,603 potential grounding accident scenarios by replaying one year's worth of VTS AIS data in our MTS simulation set-up.

From Table 2 we observe that in terms of baseline average annual oil outflow, powered grounding ranks first (about 218 m^3), next collisions (about 134 m^3) and finally drift groundings (about 9 m^3). In terms of oil outflow category, the VOI PO category ranks first (about 327 m^3 out of the total combined annual average of 361 m^3) and the IV PO ranks last (about 2 m^3). The category IV NPO ranks second to last (about 9 m^3) which is consistent with a knowledge based intuition that one might have, since most IV's carry diesel fuel. The IV PO categories and IV NPO categories only have oil outflow for the collision accidents. Most notable about the preceding analysis is that the IV NPO category oil outflow is of about the same size as that of the drift grounding category of VOI's. Percentage wise, however, both the drift grounding oil flow category and the IV NPO category comprise barely 3% of the

Table 2 Total average annual oil outflow (in m^3) separated by persistent oil (PO), non-persistent oil (NPO), VOI, IV, and accident type

in m^3	VOI PO	VOI NPO	IV PO	IV NPO	Total Outflow
Collisions	109.82	12.35	2.06	9.47	133.71
Powered Groundings	208.62	9.73	N/A	N/A	218.35
Drift Groundings	8.39	0.52	N/A	N/A	8.91
Total Outflow	326.82	22.61	2.06	9.47	360.96
in % of Total Outflow	VOI PO	VOI NPO	IV PO	IV NPO	Total Outflow
Collisions	30.42%	3.42%	0.57%	2.62%	37.04%
Powered Groundings	57.79%	2.70%	N/A	N/A	60.49%
Drift Groundings	2.32%	0.14%	N/A	N/A	2.47%
Total Outflow	90.54%	6.26%	0.57%	2.62%	100.00%

combined aggregated oil losses. The analysis in Table 2 indicates that future risk interventions may show a larger benefit by concentrating on the powered grounding and collision accident scenario types and cargo losses both in terms of crude oil and refined products.

While Table 2 provide baseline aggregate risk values for (2), it does not provide a deeper understanding of the set of accident scenarios (1) that generated it. To arrive at such an understanding, Fig. 13 displays the distribution of the combined annual average oil outflow in a geographic profile. The graphical and geographic format of Fig. 13 was used in Merrick et al. (2003) to display traffic congestion, but was enhanced to allow for displaying accident frequency and oil outflow analysis results. While Fig. 13 displays an aggregated oil outflow distribution, separate geographic profiles may be generated for all four oil loss categories in Table 2. Oil outflow losses by location and size are explained through the use of a color scale. Those grid cells within Fig. 13 that have a higher oil outflow receive a darker color than those that have less oil outflow, according to the color legend. Please note that the color legend has a non-linear scale. Its color definition is chosen such that the beginning of the yellow color range (the color next to the number 1.00) coincides with the oil outflow loss averaged over all grid cells that experience losses. In other words, those grid cells that have a color from the yellow color on and upward along the color scale in Fig. 13, exhibit a larger than average oil outflow, and those grid cells with a green color and light blue color exhibit a smaller than average oil outflow. Hence, when visually inspecting these geographic profiles from an oil outflow results perspective, one might be particularly interested in those colors that are yellow and higher.

Shifting attention to the plot in the middle of the geographic profile, one observes a further indication that the distribution of outflow of baseline accident scenarios in (1) across grid cells is highly non-linear. The horizontal axis list the percentage of grid cells that have color (and thus oil outflow) in Fig. 13 and the vertical axis displays the oil outflow volume (in m^3). The non-linear curves in this plot displays the progression in the cumulative oil outflow when ordering the grid cells by their average oil flow from largest to smallest. The color scale of the geographic profile follows a power scale that matches that non-linearity to achieve a higher color contrast amongst grid cells. Focusing on the end points of these curves, one arrives at the same baseline aggregate risk (2) conclusion previously derived from Table 2. That is, potential power grounding accident scenarios rank first in terms of total annual average oil outflow followed by collisions and next drift groundings scenarios.

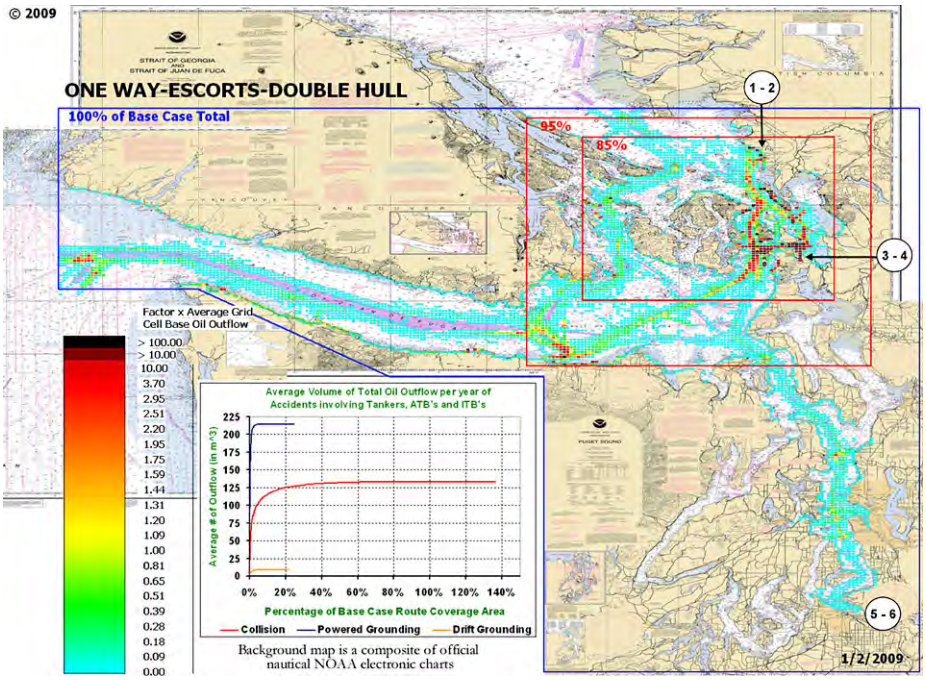

Fig. 13 Geographic oil outflow profile explaining base case system risk (1) with Fig. 1 risk interventions being operational

Percentages along the x-axis in these plots are measured relative to the total annual number of grid cells that VOI's traverse. The grid cells with color that result from collision interactions, color both the grid cell location of the VOI and the IV (see Fig. 8B). Hence, the coverage area of collisions naturally covers a larger area than the route coverage alone of VOI's and hence its end-point along the x-axis goes beyond the 100% value. We can conclude from the plot in Fig. 13 that the top 60% of the collision interaction grid cells account for almost all of the oil outflow loss due to collisions. Observe that the coverage area of powered grounding just exceeds 20% along the x-axis, i.e. indicating relatively larger oil outflows over fewer grid cells.

A concentration of oil out flow losses from potential accident scenarios is further evidenced by the two displayed red rectangles in Fig. 13. Displayed percentages in their top left corners indicate the percentage of overall baseline aggregate oil loss (360.96 m^3, see Table 2) within these areas. Hence 85% of the oil outflow across the entire area is attributed to the smaller rectangle and 95% to the larger one (which includes the smaller one). Observe from Fig. 13 that this 10% difference can be primarily attributed to the darker colored areas in the lower left corner of the larger red rectangle. This is actually the area where deep draft vessels have to "dip" southward and slow down to pick up and drop off pilots for their continued journeys.

7 An example of a risk management effectiveness analysis

To illustrate the risk management effectiveness analysis methodology in this paper, we shall apply it to evaluate the effectiveness of the three risk interventions displayed in Fig. 1 as

Average Annual Oil Outflow (nv) by Category	VOI PO	VOI NPO	IV PO	IV NPO	Total Outflow
CASE 3: TWO WAY-NO ESCORTS-SINGLE HULL	4042.33	232.32	2.77	23.22	4300.63
CASE 2: ONE WAY-NO ESCORTS-SINGLE HULL	3802.44	194.98	2.54	27.75	4027.72
CASE 1: ONE WAY-ESCORTS-SINGLE HULL	1265.07	100.21	2.06	9.47	1376.81
BASE CASE: ONE WAY-ESCORTS-DOUBLE HULL	326.82	22.61	2.06	9.47	360.96

% Change in Category from Case 3	VOI PO	VOI NPO	IV PO	IV NPO	Total Outflow
CASE 3: TWO WAY-NO ESCORTS-SINGLE HULL	100.0%	100.0%	100.0%	100.0%	100.0%
CASE 2: ONE WAY-NO ESCORTS-SINGLE HULL	94.1%	83.9%	91.8%	119.5%	93.7%
CASE 1: ONE WAY-ESCORTS-SINGLE HULL	31.3%	43.1%	74.6%	40.8%	32.0%
BASE CASE: ONE WAY-ESCORTS-DOUBLE HULL	8.1%	9.7%	74.6%	40.8%	8.4%

% Change in Category from Base Case	VOI PO	VOI NPO	IV PO	IV NPO	Total Outflow
CASE 3: TWO WAY-NO ESCORTS-SINGLE HULL	1236.9%	1027.6%	134.0%	245.1%	1191.4%
CASE 2: ONE WAY-NO ESCORTS-SINGLE HULL	1163.5%	862.5%	123.1%	293.1%	1115.8%
CASE 1: ONE WAY-ESCORTS-SINGLE HULL	387.1%	443.2%	100.0%	100.0%	381.4%
BASE CASE: ONE WAY-ESCORTS-DOUBLE HULL	100.0%	100.0%	100.0%	100.0%	100.0%

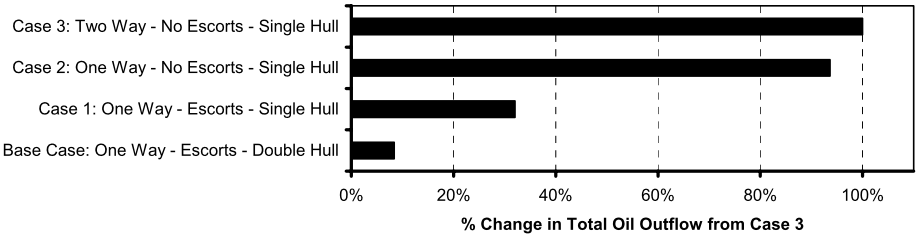

Fig. 14 Total average annual oil outflow (in m^3) separated by persistent oil (PO), non-persistent oil (NPO), VOI, IV and Sect. 7 cases

deviations from the baseline risk (1) and (2) presented in Sect. 6. Three modifications to the base case analysis described in the previous section shall be considered as separate cases. In Case 1 the double requirement is removed from the base case. In Case 2, the escorting scheme is "peeled back" from Case 1. Finally, Case 3 is constructed from Case 2 by allowing for two-way traffic in Rosario Strait. Summarizing, in Case 3 neither of the risk interventions in Fig. 1 are in place, whereas in the base case analysis of Sect. 6 all three were operational.

Figure 14 details the overall aggregate analysis results by the oil outflow categories VOI PO, VOI NPO, IV PO, IV NPO and total oil outflow by case. The middle table in Fig. 14 provides some interesting observations. Firstly, concentrating on total outflow we observe that in the base case on average only about 8% of the Case 3 oil outflow remains. Hence, the combined effectives of these three risk intervention measures resulted in about a 92% oil outflow reduction, which is impressive. The tornado diagram in Fig. 14 highlights these reductions by case. One observes from Fig. 14 that the largest reduction resulted from the implementation of the escort scheme (a reduction of over 61.7% from 93.7% to 32.0%), followed by the implementation of the double hull requirement (a reduction of 23.6% from 32.0% to 8.4%). The one-way zone implementation resulted in a relatively minor reduction (6.3% from 100% to 93.7%) due to a risk migration behavior in the MTS simulation. Even though a one-way zone reduces certain interactions in a targeted location (Rosario Strait in this case), an unintended effect of such an implementation is that traffic congestion elsewhere increases. In fact, we can observe an increase of 19.5% in the IV NPO category (which includes diesel fuel losses from interacting vessels) going from Case 3 to Case 2,

whereas we see a reduction in all other categories. Overall going from Case 3 to Case 2 the net effect of the one-way zone implementation is still an overall reduction in oil outflow of the 6.3% indicated above. Another interesting observation from the middle table is that going from Case 2 to Case 1 (which deals with the escorting scheme implementation) the oil outflows of the IV categories goes down as well (from 91.8% to 74.6% for IV PO and from 119.5% to 40.8% for IV NPO). This results from escorting vessels also providing an external vigilance component ("additional eyes on the water") and thus also results in a reduction of the collision probability per interaction with other vessels. Finally, we observe no change in the IV oil outflow categories going from Case 1 to the base case (dealing with the double hull requirement) since the double hull requirement only applies to the VOI's, not to the IV's.

We conclude the risk management effectiveness analysis by generating a geographic profile of oil outflow losses due to potential accident scenarios in (1) generated for Case 3, depicted in Fig. 15. Please note that the color scale in Fig. 15 is identical to that in Fig. 13 and therefore the two figures allow for a direct visual assessment of the change in oil outflow risk when going from the base case to Case 3. The curves in the middle of the geographic profile show a similar behavior in the comparisons across cases as the tabular analysis in Fig. 14. Moreover, we observe from these curves a similar non-linearity in the distribution of oil outflow analysis, suggesting no dramatic shift in the predominant locations of oil flow losses from case to case. This is further evidenced by the geographic profile in Fig. 15. We primarily observe a darkening of color in the smaller red rectangle and in the lower right corner of the larger red rectangle. We also see a slight darkening along the south coast line of the main waterway towards the ocean (the Strait of Juan de Fuca).

Please note that the left top blue border corner percentage of 1191% coincides with the total oil outflow percentage of Case 3 in the third table in Fig. 14. Hence, the percentages in the top left corners continue to be evaluated as percentage changes from the base case analysis described in Sect. 6. We have 1180% in the larger red rectangle and 1142% in the smaller one. Hence, overall in Case 3 one obtains:

$$\%\ \text{Oil outflow in Larger Red Square: } 1180\%/1191\% \approx 99\%,$$

$$\%\ \text{Oil outflow in Smaller Red Square: } 1142\%/1191\% \approx 96\%,$$

whereas in the Base Case scenario these percentages were 95% and 85%, respectively. Summarizing, going from Case 3 to the base case scenario risk reduced from 100% to 8.4%. Of the remaining 8.4%, however, 95% and 85% fall in the larger and smaller red square in the geographic profiles, respectively. Thus, while these three risk interventions result in an impressive risk reduction, the distribution of remaining risk is predominantly concentrated in the same overall locations, with a small shift towards the lower left corner of the larger red rectangle in Fig. 15.

8 Concluding remarks

More data is being made available electronically over time allowing for an even more accurate representation of the movement of vessel traffic and modeling of the environment within an MTS simulation. However, with the increased availability of this electronic data comes an increased time to prepare it in an electronic format that can serve as input to an MTS simulation. Despite these advances, one should always bear in mind that any simulation model is an abstraction of reality in which simplifying assumptions are often necessitated to maintain

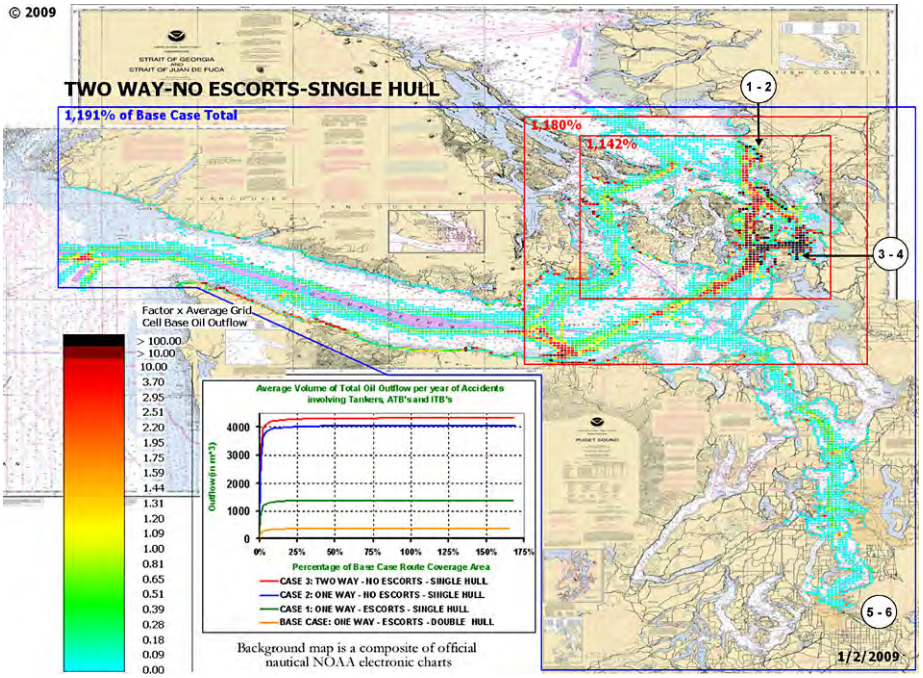

Fig. 15 Geographic oil outflow profile of explaining Case 3 system risk (1) without Fig. 1 risk interventions being operational

computational efficiency. We find that relative comparisons across accident types, across oil outflow categories and across risk intervention scenarios are particularly enlightening. We concentrate less on the absolute values of the results in our analysis comparisons.

Acknowledgements We are indebted to both referees and the editor whose comments improved the presentation and the content of an earlier version.

References

Andrews, S., Murphy, F. H., Wang, X. P., & Welch, S. (1996). Modeling crude oil lightering in Delaware Bay. *Interfaces*, *26*(6), 68–78.

Bedford, T. M., & Cooke, R. M. (2001). *Probabilistic risk analysis: Foundations and method*. Cambridge: Cambridge University Press.

Evans, D. L., Grudes, S. B., & Davidson, M. A. (2001). *United States Coast Pilot, Pacific Coast, California, Oregon, Washington and Hawaii*, Vol. 7. National Ocean Service, U.S. Department of Commerce, Washington D.C.

Fowler, T. G., & Sorgard, E. (2000). Modeling ship transportation risk. *Risk Analysis*, *20*(2), 225–244.

Golkar, J., Shekhar, A., & Buddhavarapu, S. (1998). Panama canal simulation model. In *Proceedings of the 1998 winter simulation conference* (pp. 1229–1237).

GuedesSoares, C., & Teixeira, A. P. (2001). Risk assessment in maritime transportation. *Reliability Engineering and System Safety*, *74*(3), 299–309.

Hara, K., & Nakamura, S. (1995). A comprehensive assessment system for the maritime traffic environment. *Safety Science*, *19*(2–3), 203–215.

International Maritime Organization (1995). *Interim guidelines for approval of alternative methods of design and construction of oil tankers under regulation 13F(5) of annex I of Marpol 73/78*. Resolution MEPC. 66(37), Adopted September 14, 1995.

Kaplan, S. (1997). The words of risk analysis. *Risk Analysis*, *17*(4), 407–417.
Kite-Powell, H. L., Jin, D., Patrikalis, N. M., Jebsen, J., & Papakonstantinou, V. (1996). *Formulation of a model for ship transit risk* (MIT Sea Grant Technical Report). Cambridge, MA, 96-19.
Maio, D., Ricci, R., Rossetti, M., Schwenk, J., & Liu, T. (1991). *Port needs study* (Report No. DOT-CG-N-01-91-1.2). Prepared by John A. Volpe, National Transportation Systems Center. Washington, D.C.: U.S. Coast Guard.
MAPTECH (2007). http://www.maptech.com/, last accessed: 10/10/2009.
Merrick, J. R. W. (2002). Evaluation of tug escort schemes using simulation of drifting tankers. *Simulation: Transactions of the Society for Modeling and Simulation International*, *78*(6), 380–388.
Merrick, J. R. W., van Dorp, J. R., Harrald, J., Mazzuchi, T., Spahn, J., & Grabowski, M. (2000). A systems approach to managing oil transportation risk in Prince William Sound. *Systems Engineering*, *3*(3), 128–142.
Merrick, J. R. W., van Dorp, J. R., Mazzuchi, T., & Harrald, J. (2001). Modeling risk in the dynamic environment of maritime transportation. In *Proceedings of the 2001 winter simulation conference* (pp. 1090–1098).
Merrick, J. R. W., van Dorp, J. R., Harrald, J., Mazzuchi, T., Spahn, J., & Grabowski, M. (2002). The Prince William Sound risk assessment. *Interfaces*, *32*(6), 25–40.
Merrick, J. R. W., van Dorp, J. R., Blackford, J. P., Shaw, G. L., Mazzuchi, T. A., & Harrald, J. R. (2003). A traffic density analysis of proposed ferry service expansion in San Francisco Bay using a maritime simulation model. *Reliability Engineering and System Safety*, *81*(2), 119–132.
Merrick, J. R. W., van Dorp, J. R., & Singh, A. (2005). Analysis of correlated expert judgments from pairwise comparisons. *Decision Analysis*, *2*(1), 17–29.
National Climatic Data Center (2007). http://www.ncdc.noaa.gov/oa/ncdc.html, last accessed: 10/10/2009.
National Oceanic and Atmospheric Administration (1997). *Ship drift analysis for the northwest Peninsula and the strait of Juan de Fuca* (HAZMAT Report 97-3).
National Oceanic and Atmospheric Administration (2007). http://tidesandcurrents.noaa.gov/, last accessed: 10/10/2009.
National Research Council (1986). *Crew size and maritime safety*. Washington: National Academy Press.
National Research Council (1991). *Tanker spills: Prevention by design*. Washington: National Academy Press.
National Research Council (1994). *Minding the helm: Marine navigation and piloting*. Washington: National Academy Press.
National Research Council (2000). *Risk management in the marine transportation system*. Washington: National Academy Press.
National Research Council (2001). *Environmental performance of tanker designs in collision and grounding* (Special Report 259). Marine Board, Transportation Research Board, The National Academies.
Paté-Cornell, M. E. (1990). Organizational aspects of engineering system safety: The case of offshore platforms. *Science*, *250*(4985), 1210–1217.
Pravda, M. F., & Lightner, R. G. (1966). Conceptual study of a super-critical reactor plant for merchant ships. *Marine Technology*, *4*, 230–238.
Roeleven, D., Kok, M., Stipdonk, H. L., & de Vries, W. A. (1995). Inland waterway transport: Modeling the probabilities of accidents. *Safety Science*, *19*(2–3), 191–202.
Ryan, N. K. (1998). The future of maritime facility designs and operations. In *Proceedings of the 1998 winter simulation conference* (pp. 1223–1227).
Slob, W. (1998). Determination of risks on inland waterways. *Journal of Hazardous Materials*, *61*(1–3), 363–370.
Stiehl, G. L. (1977). Prospects for shipping liquefied natural gas. *Marine Technology*, *14*(4), 351–378.
Szwed, P., van Dorp, J. R., Merrick, J. R. W., Mazzuchi, T. A., & Singh, A. (2006). A Bayesian paired comparison approach for relative accident probability assessment with covariate information. *European Journal of Operations Research*, *169*(1), 157–177.
Taggart, R. (1980). *Ship design and construction*. The Society of Naval Architects and Marine Engineers.
Trbojevic, V. M., & Carr, B. J. (2000). Risk based methodology for safety improvements in ports. *Journal of Hazardous Materials*, *71*(1–3), 467–480.
Ulusçu, O, Özbas, B., Altiok, T., & Or, I. (2009). Risk analysis of the vessel traffic in the strait of Istanbul. *Risk Analysis*, *29*(10), 1454–1472.
U.S. Coast Guard (1973). *Vessel traffic systems: Analysis of port needs* (Report No. AD-770 710). Washington, DC: U.S. Coast Guard.
U.S. Coast Guard (2008). *Incident specific preparedness review (ISPR) M/V cosco busan oil spill in San Francisco Bay*, Accessed January 2009. http://uscg.mil/foia/CoscoBuscan/CoscoBusanISPRFinal.pdf.
van de Wiel, G. (2008). *A probabilistic model for oil spill volume in tanker collisions and groundings*. Masters Thesis, Delft University of Technology, Delft, The Netherlands.

van de Wiel, G., & van Dorp, J. R. (2009). An oil outflow model for tanker collisions and groundings, *Annals of Operations Research, Special Volume on Part Security/Safety, Risk Analysis and Modeling*. doi:10.1007/s10479-009-0674-5.

van Dorp, J. R., Merrick, J., Harrald, J., Mazzuchi, T., & Grabowski, M. (2001). A risk management procedure for the Washington State ferries. *Risk Analysis*, *21*(1), 127–142.

Wang, J. (2000). A subjective modeling tool applied to formal ship safety assessment. *Ocean Engineering*, *27*(10), 1019–1035.

WXTIDE32 (2007). http://www.wxtide32.com/index.html, last accessed: 10/10/2009.